

## Where did tropospheric ozone over southern Africa and the tropical Atlantic come from in October 1992? Insights from TOMS, GTE TRACE A, and SAFARI 1992

A. M. Thompson,<sup>1,2</sup> K. E. Pickering,<sup>2</sup> D. P. McNamara,<sup>3</sup> M. R. Schoeberl,<sup>1</sup> R. D. Hudson,<sup>2,4</sup> J. H. Kim,<sup>4,5</sup> E. V. Browell,<sup>6</sup> V. W. J. H. Kirchhoff,<sup>7</sup> and D. Nganga<sup>8</sup>

**Abstract.** The seasonal tropospheric ozone maximum in the tropical South Atlantic, first recognized from satellite observations [Fishman *et al.*, 1986, 1991], gave rise to the IGAC/STARE/SAFARI 1992/TRACE A campaigns (International Global Atmospheric Chemistry/South Tropical Atlantic Regional Experiment/Southern African Fire Atmospheric Research Initiative/Transport and Atmospheric Chemistry Near the Equator-Atlantic) in September and October 1992. Along with a new TOMS-based method for deriving tropospheric column ozone, we used the TRACE A/SAFARI 1992 data set to put together a regional picture of the O<sub>3</sub> distribution during this period. Sondes and aircraft profiling showed a troposphere with layers of high O<sub>3</sub> ( $\geq 90$  ppbv) all the way to the tropopause. These features extend in a band from 0° to 25°S, over the SE Indian Ocean, Africa, the Atlantic, and eastern South America. A combination of trajectory and photochemical modeling (the Goddard (GSFC) isentropic trajectory and tropospheric point model, respectively) shows a strong connection between regions of high ozone and concentrated biomass burning, the latter identified using satellite-derived fire counts [Justice *et al.*, this issue]. Back trajectories from a high-O<sub>3</sub> tropical Atlantic region (column ozone at Ascension averaged 50 Dobson units (DU)) and forward trajectories from fire-rich and convectively active areas show that the Atlantic and southern Africa are supplied with O<sub>3</sub> and O<sub>3</sub>-forming trace gases by midlevel easterlies and/or recirculating air from Africa, with lesser contributions from South American burning and urban pollution. Limited sampling in the mixed layer over Namibia shows possible biogenic sources of NO. High-level westerlies from Brazil (following deep convective transport of ozone precursors to the upper troposphere) dominate the upper tropospheric O<sub>3</sub> budget over Natal, Ascension, and Okaukuejo (Namibia), although most enhanced O<sub>3</sub> (75% or more) equatorward of 10°S was from Africa. Deep convection may be responsible for the timing of the seasonal tropospheric O<sub>3</sub> maximum: Natal and Ascension show a 1- to 2-month lag relative to the period of maximum burning [cf. Baldy *et al.*, this issue; Olson *et al.*, this issue]. Photochemical model calculations constrained with TRACE A and SAFARI airborne observations of O<sub>3</sub> and O<sub>3</sub> precursors (NO<sub>x</sub>, CO, hydrocarbons) show robust ozone formation (up to 15 ppbv O<sub>3</sub>/d or several DU/d) in a widespread, persistent, and well-mixed layer to 4 km. Slower but still positive net O<sub>3</sub> formation took place throughout the tropical upper troposphere [cf. Pickering *et al.*, this issue (a); Jacob *et al.*, this issue]. Thus whether it is faster rates of O<sub>3</sub> formation in source regions with higher turnover rates or slower O<sub>3</sub> production in long-lived stable layers ubiquitous in the TRACE A region, 10–30 DU tropospheric O<sub>3</sub> above a ~25-DU background can be accounted for. In summary, the O<sub>3</sub> maximum studied in October 1992 was caused by a coincidence of abundant O<sub>3</sub> precursors from biomass fires, a long residence time of stable air parcels over the eastern Atlantic and southern Africa, and deep convective transport of biomass burning products, with additional NO from lightning and occasionally biogenic sources.

<sup>1</sup>NASA Goddard Space Flight Center, Laboratory for Atmospheres, Greenbelt, Maryland.

<sup>2</sup>Univ. of Maryland Joint Center for Earth System Science (JCESS), College Park, Maryland.

<sup>3</sup>Applied Research Corporation, Landover, Maryland.

<sup>4</sup>University of Maryland, Department of Meteorology, College Park.

<sup>5</sup>Now at Earth System Science Laboratory, University of Alabama, Huntsville.

<sup>6</sup>NASA Langley Research Center, Atmospheric Sciences Division, Hampton, Virginia

<sup>7</sup>INPE, São Jose de Campos, São Paulo, Brazil.

<sup>8</sup>Department of Atmospheric Physics, Marien Ngouabi University, Brazzaville, Congo.

## 1. Introduction

A seasonal maximum in tropospheric  $O_3$  extending over the south tropical Atlantic and adjacent South America and Africa was reported by Fishman and coworkers based on satellite ozone observations [Fishman *et al.*, 1986, 1991; Fishman, 1988]. Tropospheric ozone in this region peaks in the August–October period, then declines in November. During the peak period, biomass burning is intense and widespread in South America and southern Africa. The tropospheric  $O_3$  column depth may exceed 50 Dobson Units ( $1 \text{ DU} = 2.69 \times 10^{16} \text{ cm}^{-2}$ ) or more, compared to nonpolluted tropical tropospheric ozone column depths of 20–30 DU [Kirchhoff *et al.*, 1991; Cros *et al.*, 1992]. Tropical circulation patterns tend to promote tropospheric  $O_3$  accumulation off the African coast during the September–October period [Krishnamurti *et al.*, 1993]. Thus both photochemical and dynamical forces could play roles in the regional tropospheric ozone maximum.

Two IGAC/STARE (South Tropical Atlantic Regional Experiment) field programs were designed to explore  $O_3$  and the interaction of chemical and dynamical influences in the tropical South Atlantic and adjoining continents in September and October 1992. The principal aim of TRACE A (Transport and Atmospheric Chemistry Near the Equator-Atlantic), one of the GTE (Global Tropospheric Experiment) aircraft missions, was broad characterization of potential source regions in Brazil and southern Africa with an emphasis on Atlantic outflow from each continent [Fishman, 1994, Fishman *et al.*, this issue (a)]. SAFARI (Southern African Fire Atmospheric Research Initiative), with multiple aircraft and ground stations in southern Africa, focused atmospheric sampling near biomass fires, with measurements of pyrogenic emissions, biogenic fluxes, and ecological parameters [Andreae *et al.*, 1994; Lindesay *et al.*, this issue]. SAFARI overview papers appear in the work of van Wilgen *et al.*, [1996, SAFARI Book].

The TRACE A overview [Fishman *et al.*, this issue (a)] and meteorological environment [Bachmeier and Fielberg, this issue] are described elsewhere in this issue. The present paper integrates ozone observations and satellite imagery with photochemical and trajectory modeling to answer the major questions of TRACE A:

1. What is the distribution of tropospheric ozone in the south tropical Atlantic region during TRACE A? What are regional characteristics of boundary layer and free tropospheric ozone and the vertical distribution throughout the region? (section 2).

A synthesis of TRACE A and SAFARI ozone observations from satellite-based, aircraft, ground-based, and sounding platforms (detailed in references in Table 1) gives a comprehensive picture of South Atlantic basin ozone in September and October 1992. Vertical and horizontal ozone distributions are summarized with satellite-derived tropospheric column ozone to describe a broad area in early October 1992, complementary to the flight-by-flight overview of Fishman *et al.* [this issue (a)]. The picture that emerges is similar to the UV-DIAL based climatology of Browell *et al.* [this issue].

2. What is the role of transport in determining the ozone distribution? Are there links between regions of high tropospheric  $O_3$  and biomass burning with and without deep convection? (section 3).

Forward trajectories are run from fire-rich and convectively active areas of Africa and South America and backward trajectories are initiated from a broad Atlantic tropospheric  $O_3$

maximum detected in October 1992. Patterns and statistics from back trajectories initiated from fixed  $O_3$  sounding sites during TRACE A/SAFARI are used for more focused insights into ozone sources. For a large-scale dynamical interpretation the reader is referred to the tropical general circulation model study by Krishnamurti *et al.* [this issue]. Southern African climatology for the TRACE A and SAFARI period is described by Garstang *et al.* [this issue] and Tyson *et al.* [1996].

3. What is the magnitude of photochemical ozone formation based on trace gas measurements made during TRACE A and SAFARI? What are the relative contributions of natural and anthropogenic processes to CO,  $NO_x$ , hydrocarbon budgets, and to ozone formation in southern Africa and the tropical Atlantic?

A photochemical (instantaneous, "point") model used to assimilate DC-8 data indicates that the highest ozone formation rates occur in a thick mixed layer over southern Africa (section 4). This view is corroborated by point-modeling analysis of SAFARI aircraft data [Zenger *et al.*, 1996]. Details of point modeling for all TRACE A flights are given by Jacob *et al.* [this issue], who show that the upper troposphere is ozone producing throughout the South Atlantic basin with few exceptions. The major net ozone-destroying regions appear to be the middle troposphere and the marine boundary layer, as described by Heikes *et al.* [this issue]. The midtropospheric  $O_3$  lifetime is sufficient, however, that transport of ozone-enriched layers from the adjacent continents (predominantly Africa) helps maintain thick tropospheric ozone column depths over the Atlantic (>45 DU, on average, in early October 1992). Biogenic and biomass burning of NO, CO, and hydrocarbons over southern Africa were reported for SAFARI [Cofer *et al.*, this issue; Levine *et al.*, this issue, hereinafter referred to as L96; Scholes *et al.*, this issue; Zepp *et al.*, this issue], but temporal and spatial coverage varies. Thus incorporation of SAFARI fluxes into chemical models has not been attempted in this paper, although Chatfield *et al.* [this issue] have performed a two-dimensional regional model study to evaluate the natural and anthropogenic components of the South Atlantic ozone budget.

4. Can tropospheric ozone observed in the South Atlantic basin in October 1992 be explained from the photochemical and dynamic characteristics observed during SAFARI/TRACE A? What are the relative contributions of South America and Africa to ozone over the South Atlantic?

A synthesis of dynamical and photochemical features described in this study indeed explains the observed ozone distribution in southern Africa and the tropical Atlantic in October 1992 (section 5). The magnitude of the tropospheric column from south central Africa across to Brazil is 10–30 DU higher than over the nonpolluted Indian Ocean at the same latitudes [cf. Fishman *et al.*, this issue (b)]. Ozone precursors are sufficiently abundant in stable layers over southern Africa and the Atlantic that rates of 1–2 ppbv  $O_3$ /d formation build up 20–30 DU throughout the upper troposphere in 1–2 weeks. Back trajectories from the central Atlantic and from Ascension, Namibian (Okaukuejo), and Pretoria (Irene) sounding sites point to Brazil as the source of middle-upper level ozone during TRACE A/SAFARI. This suggests a mechanism in which biomass burning emissions are pumped into the upper troposphere by deep convection, a process confirmed in flight 6 (see our case study paper, Pickering *et al.*, this issue (a)). In the boundary layer, closer to  $O_3$  precursor sources, typical  $O_3$

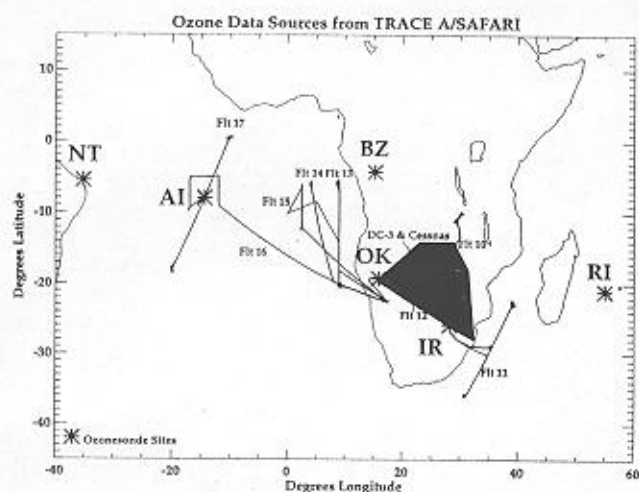


**Figure 1.** Maps showing staging sites for SAFARI/TRACE A aircraft and major fixed experimental locations: AI, Ascension; BZ, Brazzaville; NT, Natal, Brazil; OK, Okaukuejo; IR, Irene (Pretoria); RI, Réunion Island. SAFARI aircraft sampling region (shaded) applies from September 16 to October 6. TRACE A flights (numbered) took place from October 6 to 22, 1992.

lifetime is  $\sim 1$  week, but 5–15 ppbv  $O_3$ /d formation in slowly recirculating air masses can build up 10 DU or more in a week.

Throughout this paper, illustrative examples are used from other modeling studies (especially *Jacob et al.* [this issue] and *Pickering et al.* [this issue (a)]) and data analyses. Air mass classifications given by *Browell et al.* [this issue], *Gregory et al.* [this issue], and J. E. Collins et al. (personal communication, 1996, hereinafter referred to as C96) are consistent with our overview of ozone, as are various interpretations of the odd nitrogen budget described by *Singh et al.* [this issue], *Smyth* [this issue], and *Talbot et al.* [this issue]. Our objective is to present an integrating framework for all these studies and to show that the TRACE A science team answered most of the questions it set out to investigate.

## 2. Tropospheric Ozone in Southern Africa and the Atlantic During TRACE A/SAFARI

Tropospheric ozone climatology over the Atlantic and southern Africa during the southern hemisphere biomass burning season was greatly augmented by TRACE A and SA-

FARI. Figure 1 shows locations of fixed  $O_3$  sites and staging points for airborne ozone measurements in this region. Ozone instruments are listed in Table 1 and fixed site coordinates are in Table 2. Three of the Ascension sounding sites (Ascension, Brazzaville, Irene (Pretoria)) were operated for 2–3 years prior to TRACE A and SAFARI 1992 [*Cros et al.*, 1992; *Fishman et al.*, 1992; *Thompson et al.*, this issue]; Okaukuejo (Etosha Park, Namibia) was a SAFARI intensive site. INPE (the Brazilian Agency for Space Research) and TRACE A cosponsored soundings in Brazil, at Natal (which has operated since 1978) [*Kirchhoff et al.*, 1991], Porto Nacional, and Cuiabá. With an  $O_3$ -sounding program begun on Réunion (21°51'S, 55°28'E) in September 1992 [*Baldy et al.*, this issue], 1992 ozone soundings spanned the range of the satellite-sensed maximum.

Reference data for surface  $O_3$  in southern Africa are collected at the Cape Point monitoring site [*Brunke et al.*, 1990; *Scheel et al.*, 1994]. These are not significantly different from the first  $O_3$  measurements in the region [*Fabian and Pruchniewicz*, 1977].

The altitude coverage of the aircraft  $O_3$  data varies. On TRACE A the NASA DC-8 routinely covered a range from 0.3 to 12 km. Figure 1 shows two source characterization flights out of Johannesburg and one sortie to sample outflow over the Indian Ocean (flights 10–12). Four flights from Windhoek (flights 13–17) characterized outflow over the Atlantic from Africa and South America. For SAFARI 1992, high-frequency ozone sampling was made below 4 km in the shaded region (Figure 1) from Cessnas at Victoria Falls and Kruger Park and from a DC-3 operating in a survey mode from September 20 to October 6, 1992 [*Harris et al.*, this issue; *Zenker et al.*, 1996]. A Learjet took  $O_3$  profiles in early October simultaneously with the DC-3 [*Jury et al.*, this issue; *Diab et al.*, this issue (b)].

### 2.1. Ozone From Soundings and Aircraft

Figure 2 shows integrated tropospheric ozone from 10-min averages of the UV-DIAL  $O_3$  sensor onboard the DC-8 [*Browell et al.*, this issue] for flights 10–17 (October 6–22, 1992). The UV-DIAL tropospheric column  $O_3$  amounts equatorward of 15°S, always  $>44$  DU, are similar to the TOMS-derived ozone column depths in corresponding locations (section 2.2). The limited African data (squares in Figure 2, from flights 10 and 12) do not stand out in tropospheric  $O_3$  column amount from the Atlantic data. However, a latitude gradient, most pronounced between 15°S and 20°S (decreasing integrated  $O_3$  south of 15°S), appears over the Atlantic and African continent. Nearly all the fires detected from the advanced very high

**Table 1.** Aircraft Ozone Measurements on TRACE A and SAFARI 92

Method (Instrument)	Platform	Staging Location	Other Species
UV-DIAL, elec. chem.	DC-8 <sup>a</sup>	Johannesburg, Windhoek	CO, CO <sub>2</sub> , CH <sub>4</sub> , HCHO, NMHC, NO, NO <sub>2</sub> , NO <sub>x</sub> , HNO <sub>3</sub> , H <sub>2</sub> O <sub>2</sub> , CH <sub>3</sub> OOH, PAN, UV, P, T, rH, winds
KI wet chem. (ECC) C <sub>2</sub> H <sub>2</sub> Cl (CSI 2000)	Cessna-206 <sup>b</sup>	Victoria Falls	CO <sub>2</sub> , P, T, rH
UV (Thermo E. 49S)	Cessna-310 <sup>c</sup>	Kruger Park	CO, CO <sub>2</sub> , CH <sub>4</sub> , NMHC, NO <sub>x</sub> , P, T, rH
UV (Thermo E. 49) SCL (Scintrex)	DC-3 <sup>d</sup>	Multiple from 15° to 30°S	CO, CO <sub>2</sub> , CH <sub>4</sub> , HCHO, NMHC, NO, NO <sub>2</sub> , NO <sub>x</sub> , particles (size and composition), P, T, rH
UV (Dasibi)	Learjet <sup>e</sup>	Namibia	

<sup>a</sup>*Browell et al.* [this issue] and G. Gregory (NASA Langley).

<sup>b</sup>F. X. Meixner (Max Planck Institute, Mainz).

<sup>c</sup>G. Helas (Max Planck Institut).

<sup>d</sup>M. O. Andreae et al. (Max Planck Institut).

<sup>e</sup>*Jury et al.* [this issue].

**Table 2.** Location of SAFARI/TRACE A O<sub>3</sub>-Observing Sites

Site	Abbreviation	Location		
		Latitude	Longitude	Altitude, m
Natal, Brazil	NT	5°31'S	35°13'W	42
Porto Nacional, Brazil	PN	10°42'S	48°24'W	270
Cuiaba, Brazil	CU	15°36'S	56°06'W	240
Ascension Island	AI	8°00'S	14°00'W	91
Brazzaville, Congo	BZ	4°17'S	15°15'E	314
Victoria Falls, Zimbabwe	VF	18°10'S	25°80'E	1062
Okaukuejo (Etosha Park), Namibia	OK	19°11'S	15°55'E	1162
Rooikop, Namibia	RK	22°59'S	14°38'E	88
Tshokwane (Kruger Park), South Africa	KP	24°58'S	31°35'E	290
Pretoria, South Africa	IR	25°44'S	28°11'E	1347
(Irene since 1991)		25°52'S	28°13'E	1523
Cape Point, South Africa <sup>a</sup>	CP	34°13'S	18°17'E	
Réunion Island <sup>b</sup>	RI	21°51'S	55°28'E	200

TRACE A archive, NASA Langley. See Kirchhoff *et al.* [this issue] for Brazil, Nganga *et al.* [this issue] for Brazzaville, Diab *et al.* [this issue (a, b)] for Okaukuejo.

<sup>a</sup>Réunion and Cape Point independent of SAFARI/TRACE A; monitoring began at Cape Point in 1978; Réunion program began in September 1992 [Baldy *et al.*, this issue].

resolution radiometer (AVHRR) during this period were between 5° and 20°S. Figure 2 shows that integrated tropospheric O<sub>3</sub> over the Indian Ocean (diamonds, from flight 11) is lower than over the Atlantic, 42 DU over the Indian Ocean versus 49 DU north of 20°S on flights 13–17 over the Atlantic, but this is a limited sampling. Some of the difference is also due to a lower tropopause on flight 11, which included clean air masses as well as O<sub>3</sub>-rich air recirculated from Africa.

Further evidence for a latitude gradient in tropospheric column O<sub>3</sub> during TRACE A comes from the sounding record in September and October 1992. Figure 3 summarizes integrated tropospheric O<sub>3</sub> from six sounding sites during this period. The three sites between 0° and 10°S (Figure 3a, Natal, Brazzaville, and Ascension) are, on average, greater in tropospheric O<sub>3</sub> column depth than the sites south of 15°S. The weighted mean is 50 DU for sites in Figure 3a and 41 DU for sites in Figure 3b. Ascension and Natal have uniformly greater tropospheric column O<sub>3</sub> because they are consistently downwind of biomass burning, with relatively rapid transit times from source regions (section 3, Olson *et al.* [this issue]). Brazzaville, Okaukuejo, and Réunion had at least one sounding with integrated tropospheric O<sub>3</sub> at nonpolluted values (<35 DU).

Soundings and aircraft data alike show three features in O<sub>3</sub> distributions over southern Africa and the Atlantic: (1) A well-mixed layer of moderately aged (i.e., not adjacent to fresh fires) air to 4 km, with typical O<sub>3</sub> mixing ratios 60–100 ppbv, was ubiquitous on TRACE A DC-8 and SAFARI DC-3 flights over southern Africa (Figure 4). (2) Thin layers (a few tens meter) of high O<sub>3</sub> (90 ppbv or greater) were encountered at each sounding site (Figure 5) and on nearly every aircraft ascent or descent [Zenker *et al.*, 1996], indicating stable conditions. Constituent ratios indicated variable ages of the air masses [Gregory *et al.*, this issue]. (3) UV-DIAL sampling on the DC-8 revealed a remarkably persistent layer of high O<sub>3</sub> accompanying O<sub>3</sub> precursors in the middle and upper troposphere [Browell *et al.*, this issue, flight 13; Thompson *et al.*, 1996, Figure 7; Diab *et al.*, this issue (b)]. Between the high-ozone layers, the regime is highly variable. For example, 10-min-averaged O<sub>3</sub> profiles from the UV-DIAL instrument on almost any TRACE A flight over or near Africa (flights 10–17)

showed both background O<sub>3</sub> (<50 ppbv) and polluted concentrations above the haze layer [Browell *et al.*, this issue].

One fixed site where biomass burning effects on ozone were detected was Victoria Falls, where surface and aircraft measurements coincided on September 25 and 26, 1992 [Meixner and Helas, 1994]. These were the highest O<sub>3</sub> values recorded by the DC-3 in its sampling periods, which occurred from September 24 to 28, 1992, and from October 1 to 6, 1992. Surface ozone mixing ratios on September 25 and 26 were also the highest during the 6-week SAFARI observing period at Victoria Falls. Back trajectories from Victoria Falls showed good correlation between ozone variations and AVHRR fire counts [Meixner and Helas, 1994].

Most DC-3 and DC-8 sampling locations, as well as the sounding sites, were not in active burning regions and it is

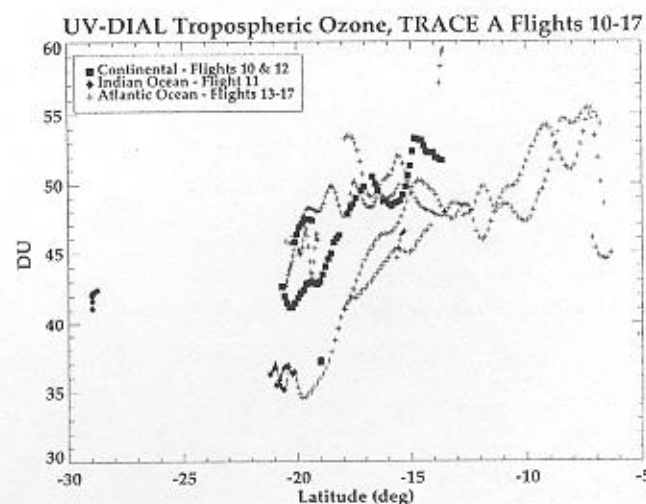


**Figure 2.** Total O<sub>3</sub> column integrated from UV-DIAL instrument versus latitude for flights originating in Africa (Figure 1). South of 15°S, tropopause height decreases rapidly, accounting for some of gradient, but trend toward greater O<sub>3</sub> toward equator is consistent with satellite-derived tropospheric O<sub>3</sub> and with soundings (compare Plate 1 and Figure 3).

important to note that biogenic  $O_3$  formation (from natural  $NO_x$ , CO, and NMHC sources) may have occurred during TRACE A along with  $O_3$  production from biomass burning. This would have been most noticeable in southern African areas where savanna burning waned in September. Biogenic CO and NO fluxes were measured on SAFARI [Zepp *et al.*, this issue; L96] and wetting of soils, even from a very light rain, increased  $NO_x$  enough to be detectable from aircraft [Harris *et al.*, this issue]. However, not enough data were collected to quantify sources, and the impact of biogenic sources on ozone during TRACE A cannot be evaluated.

## 2.2. Tropospheric Column Ozone From TOMS

A more comprehensive regional picture of tropospheric ozone during SAFARI/TRACE A is derived from the TOMS satellite instrument [Thompson *et al.*, this issue (a), 1996]. As suggested by ozonesondes and aircraft sampling, tropospheric

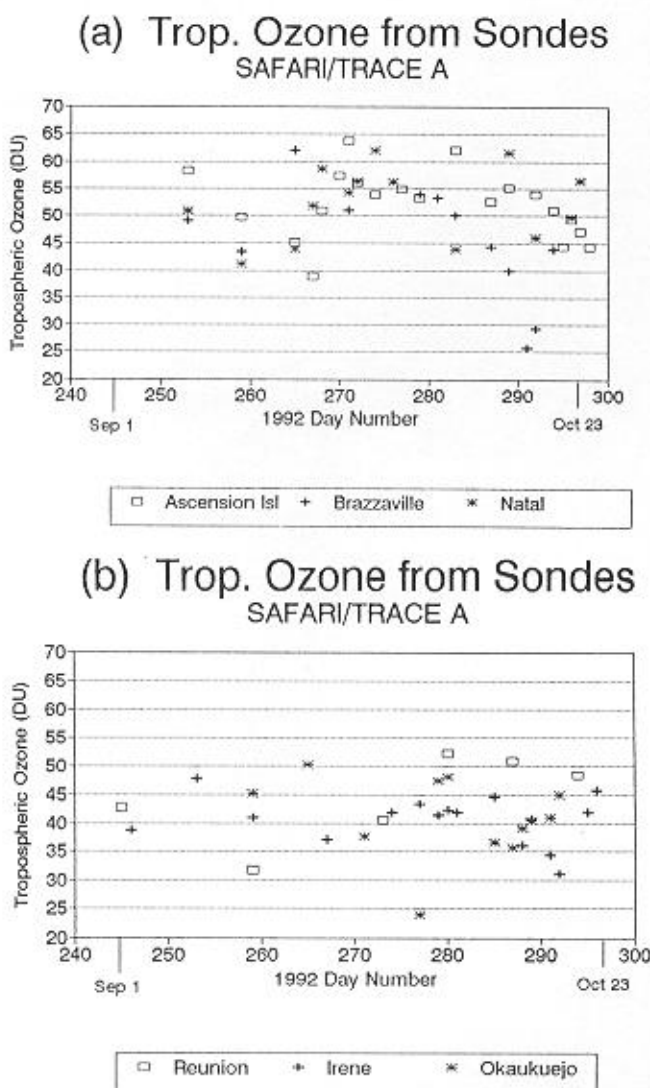


**Figure 3.** Integrated tropospheric  $O_3$  over five fixed TRACE A/SAFARI sites and Réunion Island in September–October 1992. (a) Ascension, Brazzaville, and Natal; (b) Réunion, Irene, Okaukuejo. Details on African soundings are described by Nganga *et al.* [this issue], Diab *et al.* [this issue (b)]; Brazilian soundings are described by Kirchhoff *et al.* [this issue]. See Baldy *et al.* [1996] for Réunion sounding details.

## Ozone Profiles SAFARI'92/DC-3: Flight 7, Sept 24

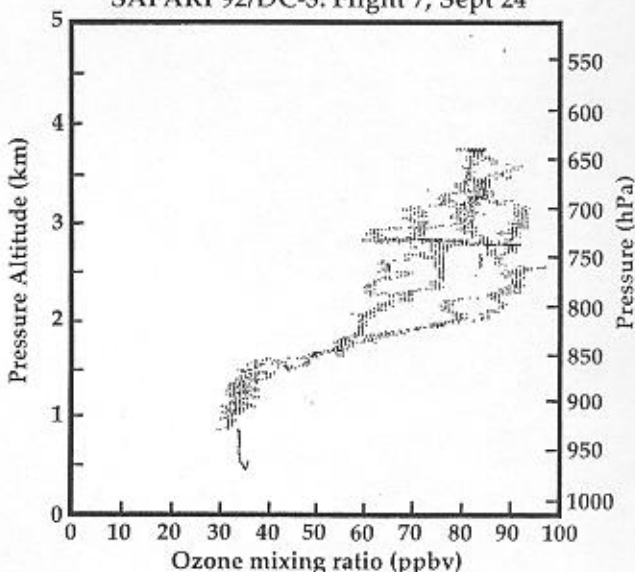


**Figure 4.** DC-3 ozone profiles from SAFARI survey in southern Africa, September 24–28, 1992. Layers with 10-s data from one flight are shown.

column ozone (Plate 1) in localized areas from South America across the Atlantic and Africa exceeds 40 DU. The map in Plate 1 is an average over the period October 6–21, 1992, derived from high-density TOMS radiances (Nimbus 7/TOMS, version 6) by Kim *et al.* [this issue]. Comparison with averaged integrated ozonesonde data from Natal, Ascension, and Brazzaville during this period shows agreement within 5% (the uncertainty in the satellite-based ozone column is 5 DU). Some of Africa is under too much cloud cover for reliable processing (gaps in Plate 1) and much of the African area north of the equator shows tropospheric column  $O_3$  close to nonpolluted levels over the western Indian Ocean. The lower  $O_3$  amount is consistent with the seasonality of 1992 biomass burning in eastern equatorial Africa, which AVHRR-derived fire counts show is nearly ended by October [Justice *et al.*, this issue]. The 16-day  $O_3$  distribution from Plate 1 is given in Table 3.

The mean difference between column-integrated ozone from the September–October 1992 soundings at Ascension and Brazzaville is 7 DU (section 2.1). Thus these sites might be representative of the Atlantic–Africa gradient shown in Table 3.

Plate 1 has been compared to the corresponding 16-day average from the TOMS/SBUV daily tropospheric ozone maps of Fishman *et al.* [this issue (b)]. Differences in the two maps are  $\sim 5$  DU over the Atlantic; both methods agree with Brazzaville, Natal, and Ascension ozonesondes within stated uncertainties. Both Fishman *et al.* [this issue (b)] and Kim *et al.* [this issue] techniques use version 6 TOMS data but with three differences: (1) Kim *et al.* [this issue] make a cloud correction for total  $O_3$  as described by Thompson *et al.* [1993] and Hudson *et al.* [1995]; (2) modified overland retrieval from TOMS radiances in the work of Kim *et al.* [this issue] uses Ascension and Brazzaville pre-TRACE ozone profiles as in the work of Hudson *et al.* [1995]; this remedies the tendency to underestimate total  $O_3$  when substantial ozone is below 500 mbar; (3) assumed “background” or equatorial Indian Ocean tropospheric ozone column amount. The Kim *et al.* [this issue] value of 26

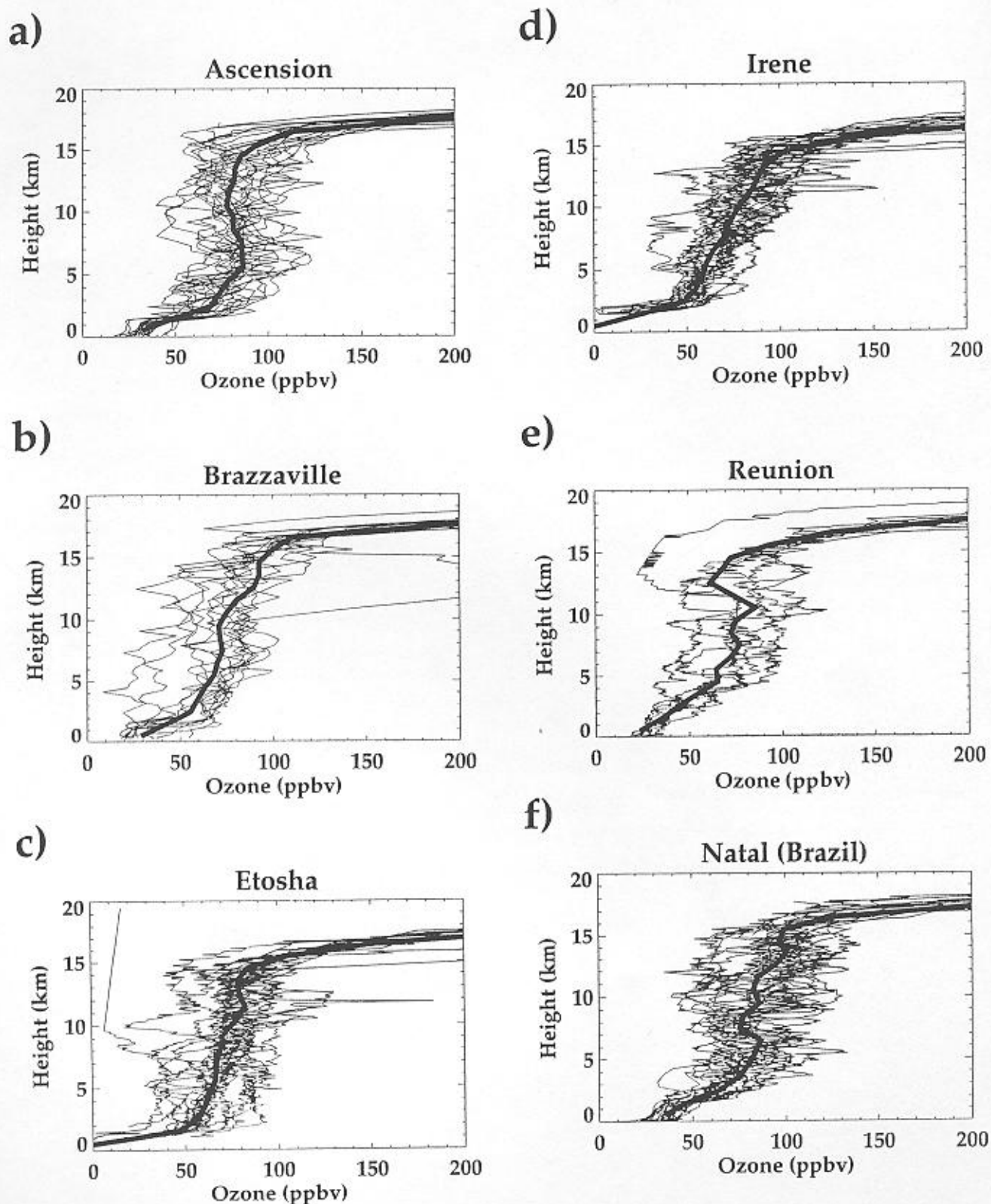
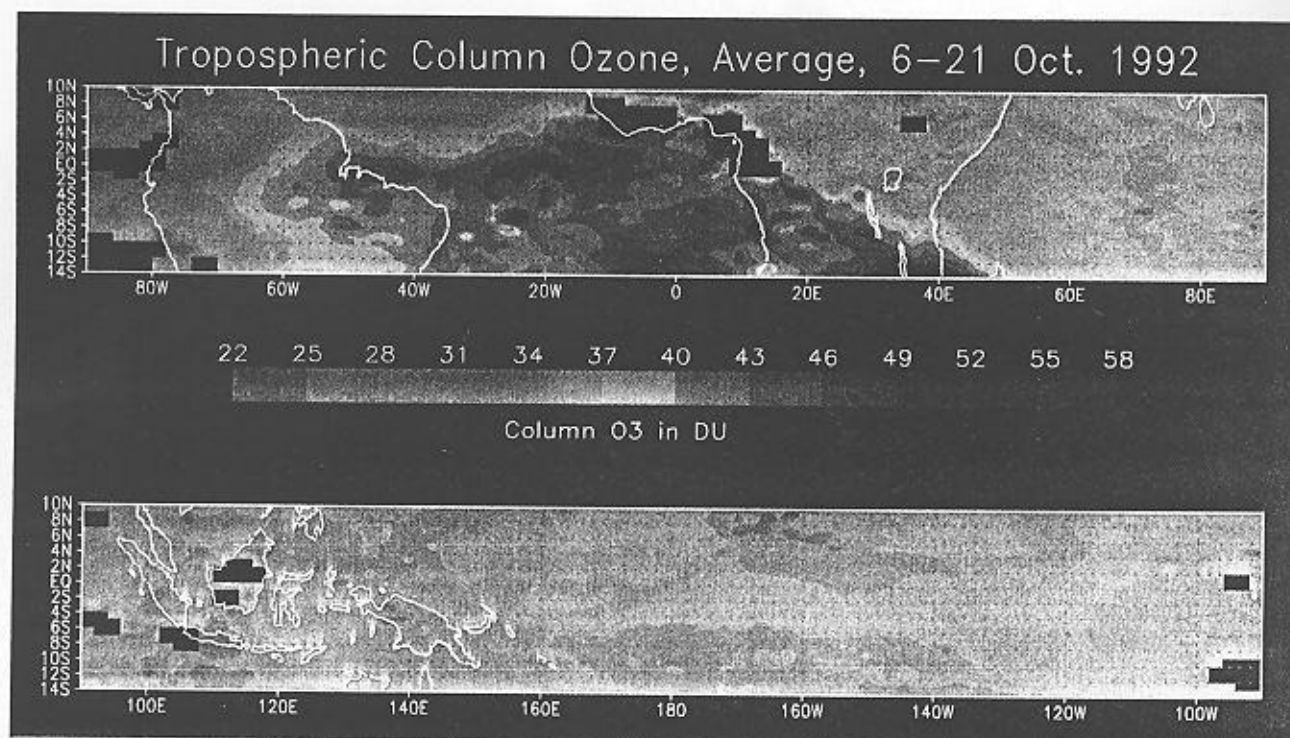


Figure 5. Ozone soundings during September–October 1992. Mean, in 1-km intervals, is thick solid line. (a) Ascension Island ( $n = 20$  sondes), (b) Brazzaville ( $n = 12$ ), (c) Etosha (Okaukuejo ( $n = 12$ )), (d) Irene ( $n = 16$ ), (e) Réunion ( $n = 7$ ), (f) Natal, Brazil ( $n = 14$ ). Natal soundings are, on average, 10–20 ppbv greater than the 1982–1991  $O_3$  climatology [Kirchhoff *et al.*, this issue].



**Plate 1.** Tropospheric column  $O_3$  derived from TOMS high-density  $O_3$  data by Kim *et al.* [this issue], averaged over 16 days in October 1992. Total ozone is derived with corrections for Mount Pinatubo aerosol, scan bias, and variable efficiency of lower tropospheric  $O_3$  over surfaces of differing albedo. Clean-air profiles and neglect of nonunity tropospheric retrieval efficiency can lead to 15–20 DU errors in total  $O_3$  when archived version 6 TOMS is used to deduce tropospheric  $O_3$  [Hudson *et al.*, 1995]. A comparison of ozonesondes during October 6–21, 1992, and the satellite product (in parentheses) shows good agreement: Ascension = 52 DU (48 DU); Brazzaville = 40 DU (38 DU); Natal = 48 DU (46 DU).

DU is closer to the TOMS-SAGE-based climatology [Fishman *et al.*, 1990] than the new TOMS-SBUV background of 38 DU [Fishman *et al.*, this issue (b)]. We take the 26 DU value because it agrees with the minimum TRACE A period soundings at Brazzaville (26 DU) [Nganga *et al.*, this issue] and Okaukuejo (24 DU at 20°S). The Kim *et al.* [this issue] method is based on high-density TOMS data (more than twice the resolution of archived TOMS), which is preferable for a focused field study, although it is limited to within 15° of the equator.

### 3. "Where Did the Ozone Come From?": Role of Dynamics

We used several approaches to examine the dynamical origins of tropospheric  $O_3$  over southern Africa and the Atlantic during TRACE A: time versus longitude diagrams of ozone (section 3.1) and trajectory analysis. Although individual back trajectories are used in nearly all TRACE A papers to interpret species correlations and the origin of air masses along

DC-8 flight tracks, our study makes the most extensive use of trajectories for characterizing larger-scale climatology and interpreting ozone over the entire TRACE A and SAFARI study areas. First, origins of parcels entering the broad Atlantic ozone maximum defined by satellite (Plate 1) are determined with back trajectories (section 3.2). Next, forward trajectories are run from potential source regions, i.e., fire-active areas in southern Africa and regions of South America and Africa affected by deep convection (sections 3.2 and 3.3). Finally, back trajectories for each day of ozonesonde launch at the six sounding sites (Figure 1) give more insight into origins and flow patterns associated with representative ozonesonde profiles (section 3.4). The picture obtained for south central southern Africa is similar to that reported by SAFARI investigators, although we use a different type of model and consider more upper tropospheric flows than Garstang *et al.* [this issue] and Tyson *et al.* [1996]. Our results are in good agreement with detailed circulation patterns described for individual stations: Olson *et al.* [this issue], Swap *et al.* [this issue] for Ascension; Baldy *et al.* [this issue] for La Réunion; Diab *et al.* [this issue (a, b)], Garstang *et al.* [this issue], and Zunckel *et al.* [this issue] for Okaukuejo.

Isentropic trajectories are used despite lack of explicit vertical motion. Note that the TRACE A trajectory intercomparison [Pickering *et al.*, this issue (b); Fuelberg *et al.*, this issue] concludes that there are insufficient data to establish a definite preference for the kinematic approach used at Florida State [Fuelberg *et al.*, this issue], the University of Virginia [Garstang *et al.*, this issue], and the University of the Witwatersrand

**Table 3.** Summary of TOMS-Derived Tropospheric Ozone

Location	(Longitude, Latitude)	Mean Tropospheric $O_3$ , DU
South America	(75°W–40°W, 0–14°S)	40
Atlantic	(40°W–12°E, 0–14°S)	47
Southern Africa	(12°E–50°E, 0–14°S)	40

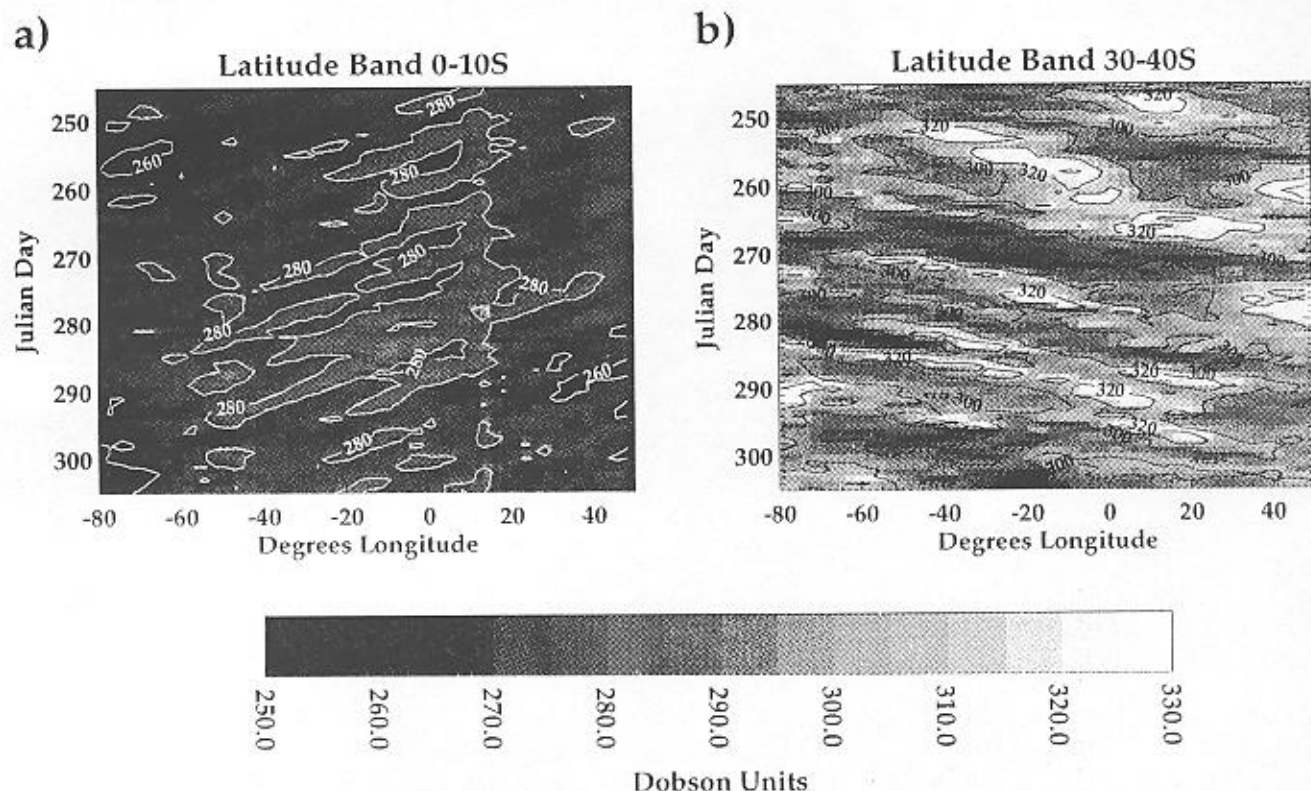


**Figure 6.** Time-longitude band (Hovmöller) plots for TOMS total  $O_3$  in September and October 1992 (days 245–305). Based on corrected  $O_3$  over Atlantic marine stratocumulus [Thompson *et al.*, 1993]; continental values are standard gridded TOMS  $O_3$  (version 6) with possible underdetection of low-level tropospheric  $O_3$ . Each gridded value averaged over a  $2^\circ$  longitude band between (a)  $0^\circ$  and  $10^\circ$ S; (b)  $30^\circ$  and  $40^\circ$ S. At  $0^\circ$ – $10^\circ$ S,  $O_3$  maxima (280 and 260 DU contours) move diagonally from NE to SW, indicating easterly flow.

[Tyson *et al.*, 1996] or isentropic trajectories used at GSFC (this paper) [Pickering *et al.*, this issue (a, b)] and Langley [Bachmeier and Fuelberg, this issue]. Errors are minimized by running multiple trajectories. Although uncertainties in any one trajectory increase with time, a tighter cluster suggests greater certainty. We use clusters of trajectories initialized at specific sampling sites. For larger areas, trajectories are initialized and run for multiple days over an appropriate grid. Thus trajectories from “convectively active” regions refer to initiations from a general region. When trajectories are run for specific locations, e.g., northeastern Brazil in the work of Pickering *et al.* [this issue (a)], postconvective, upper tropospheric initializations attempt to maintain validity of the isentropic assumption. Note that much tropical convection is sub-grid-scale and would not be captured in kinematic models either.

### 3.1. Hovmöller Plots of Total Ozone

To the extent that day-to-day total  $O_3$  variations are dominated by tropospheric  $O_3$  changes in the equatorial Atlantic during the savanna burning season [Fishman *et al.*, 1986], longitude versus time [Hovmöller, 1949] plots can be used to identify tropospheric ozone transport features for the SAFARI/TRACE A period [Thompson *et al.*, this issue]. Figure 6a shows a distinct easterly motion in the band from  $0^\circ$  to  $10^\circ$ S. Slopes of  $O_3$  maxima suggest a transit time from western Africa ( $15^\circ$ – $20^\circ$ E) to the central Atlantic of 4–7 days. This is consistent with middle to lower troposphere wind speeds for this area [Diab *et al.*, this issue (b); Pickering *et al.*, this issue (b)]. Between  $20^\circ$  and  $30^\circ$ S (not shown) [see Thompson *et al.*,

this issue] the Hovmöller plot shows no definite pattern. This is not surprising, given that the center of the Atlantic anticyclone migrates within the  $15^\circ$ – $25^\circ$ S band, leading to complex flows [Garstang and Tyson, 1996]. At higher latitudes ( $30^\circ$ – $40^\circ$ S, Figure 6b), however, the flow appears to be faster and clearly westerly. These transport patterns are typical of the meteorology during SAFARI/TRACE A [Bachmeier and Fuelberg, this issue; Garstang *et al.*, this issue].

### 3.2. Satellite Ozone and Fire Counts: Trajectory Analysis

The Hovmöller plots are consistent with a trajectory climatology based on regions of high tropospheric  $O_3$ , active fires, and deep convective outflow. Figure 7a shows fire distributions over southern Africa. Three regions in Angola (area 1), northern Zambia (area 2), and Mozambique (area 3) are active, although Figure 7b shows a sharp falloff in number of fires over the course of TRACE A.

For analysis of the broad tropospheric ozone maximum during TRACE A (Plate 1), back trajectories are run from the location of maximum tropospheric column  $O_3$ . An array of regularly spaced points within the region bounded by  $0^\circ$ – $35^\circ$ W,  $2^\circ$ – $22^\circ$ S is used to initialize 8-day trajectories every day from October 6 to 21, 1992. We use the Goddard isentropic trajectory model [Schoeberl *et al.*, 1992] with gridded ECMWF (European Center for Medium-Range Weather Forecasting) winds at four potential temperature surfaces, corresponding approximately to 700, 500, 300, and 150 mbar. Hourly parcel locations along 8-day trajectories used to construct the distribution shown in Plate 2 show two prominent features. From



lower to higher altitudes, trajectory origins switch from east (Africa) to west (South America). At the highest level (Plate 2d) only a few percent of the trajectories enter the central Atlantic from the east. Second, the greatest concentration of air parcels reaching the boxed region from the east at lower altitudes ( $\theta = 312$  K and 326 K) were within the box or the nearby Atlantic eight days earlier. Most parcels had not been over Africa eight days prior and very few parcels had origins south of 15°S. Individual trajectories show that recirculation occurred near the ozone maximum because the anticyclone centered at 20°S and 15°W suppressed outflow from Africa to the eastern Atlantic [Bachmeier and Fuelberg, this issue].

Similar dynamical features are reflected in forward trajectories run from fires within three regions of southern Africa (Plate 3a). These trajectories were started in clusters on individual days from October 1 to 15, 1992, at ~700 mbar and run for 8 days. The distribution of hourly points (summed within a  $1^\circ \times 1^\circ$  grid) shows that (1) low-moderate winds and anticyclonic motions in the southern Atlantic-western African region keep most air masses from the highest-fire region (region 2) over or near the African continent (Plate 3a, 3c); (2) air parcels from high-fire regions in Angola (box 1) exit to the west in a small stream north of the anticyclone or head toward the Indian Ocean in the westerlies; (3) almost none of the air parcels from Mozambique fires reached the Atlantic within 8 days. Individual trajectories from Mozambique show recirculation near the source or parcels streaming over the western Indian Ocean (Plate 3d). Note elevated  $O_3$  mixing ratios in the Réunion soundings above 4 km (Figure 5e, Réunion). Westerly flow of air parcels enriched by biomass burning south of 15°S has been noted by Garstang *et al.* [this issue], who estimate that only 4% of air parcels south of 18°S leave Africa toward the Atlantic.

Low-level forward trajectories from South American fires were not run because daily fire maps were not available. All Brazilian sounding sites show an impact of Brazilian biomass burning inputs [Kirchhoff *et al.*, this issue], but for the Atlantic and southern African ozone budgets of primary interest, low and midtropospheric  $O_3$  was dominated by African fires. This was even the case at Natal, Brazil (section 3.4).

### 3.3. Forward Trajectories From Convective Regions

There is strong evidence from tracers that biomass fires supply most of the  $O_3$  precursors ( $CO$ , hydrocarbons, and  $NO_x$ ) detected throughout the South Atlantic basin [Gregory *et al.*, this issue; Singh *et al.*, this issue; C96]. The mixed layer extends to 4 km maximum in southern Africa during TRACE A so that shallow and deep convection could supply  $O_3$  and the precursor gases to the easterlies for transport to the Atlantic. Flight 6 [Pickering *et al.*, this issue (a)] and related observations in Brazil [Kirchhoff *et al.*, this issue; Pereira, this issue; Smyth *et al.*, this issue] as well as air mass classification of UV-DIAL data [Browell *et al.*, this issue] give further proof that deep convection injects  $O_3$  precursors from the boundary layer to the upper troposphere, adding significantly to the  $O_3$  burden. Ozone formation from lightning-derived  $NO$  was also significant during TRACE A. Thus a trajectory climatology from regions of deep convection defines the likely extent of these processes.

We used monthly ISCCP cloud type statistics and NMC Climate Diagnostics Bulletin [National Meteorological Center (NMC), 1992] maps of outgoing longwave radiation and precipitation to identify regions of deep convection during Sep-

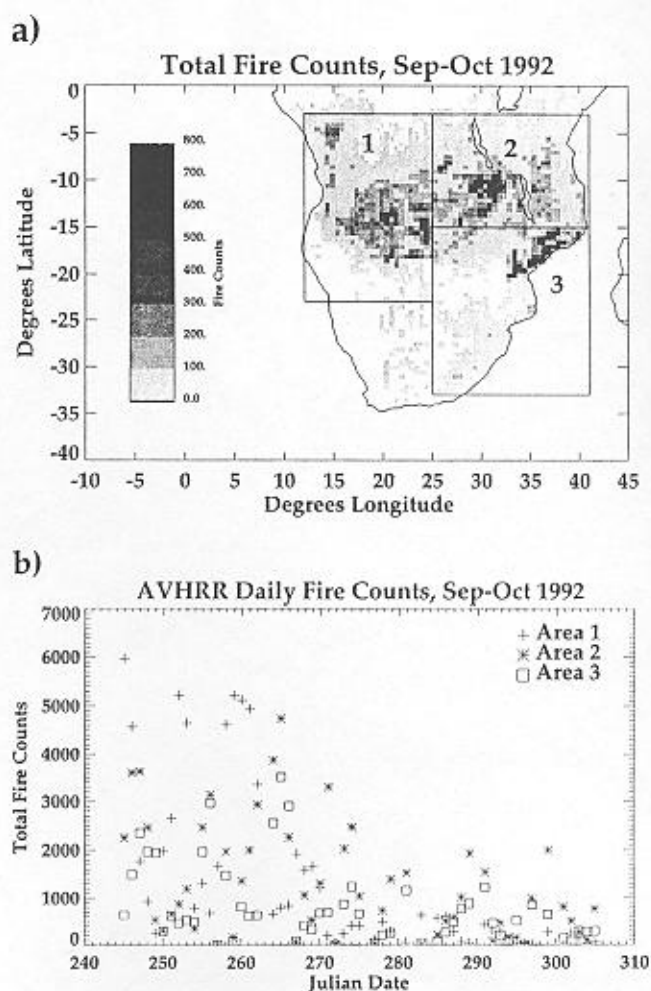


Figure 7. (a) Total AVHRR-derived fire counts for September and October 1992. Not every day has complete coverage due to missing data, clouds and hot surfaces; data loss greatest in 0°–10°S band. Fires maximize between 10° and 20°S [Justice *et al.*, this issue]. (b) Daily fire frequency in three regions delineated in Figure 7a; note days with missing data.

tember and October 1992 [cf. Kirchhoff *et al.*, this issue]. For the period of most TRACE A flights (September 25 to October 20), forward trajectories were initialized daily at grid points (white, pluses) shown in Plate 4. Plate 4a shows the distribution of points from South America (hourly parcel locations for 8 days in each  $1^\circ \times 1^\circ$  grid). Plate 4b shows the distribution of points along parcels from convective regions of Africa.

The most pronounced features in the flow from South America are (1) flow to E/SE toward Africa, with many parcels passing over the Natal, Ascension, and African sounding sites; (2) high speeds compared to lower-level flows illustrated in Plate 2. Flows from convective regions of Africa, such as lower-level flows from biomass burning regions, are concentrated over the continent, but parcels also head toward the Atlantic and Indian Oceans. Back trajectories from South Atlantic DC-8 flights 13–17 are consistent with flows from active fire and convection regions [Gregory *et al.*, this issue; C96].

### 3.4. Origins of Ozone From Soundings: Back Trajectories

A systematic approach to ozone origins was made using trajectory analysis at the sounding sites. Table 4 gives mean

## Back Trajectory Parcel Distribution 6-21 Oct 1992 Ozone Peak

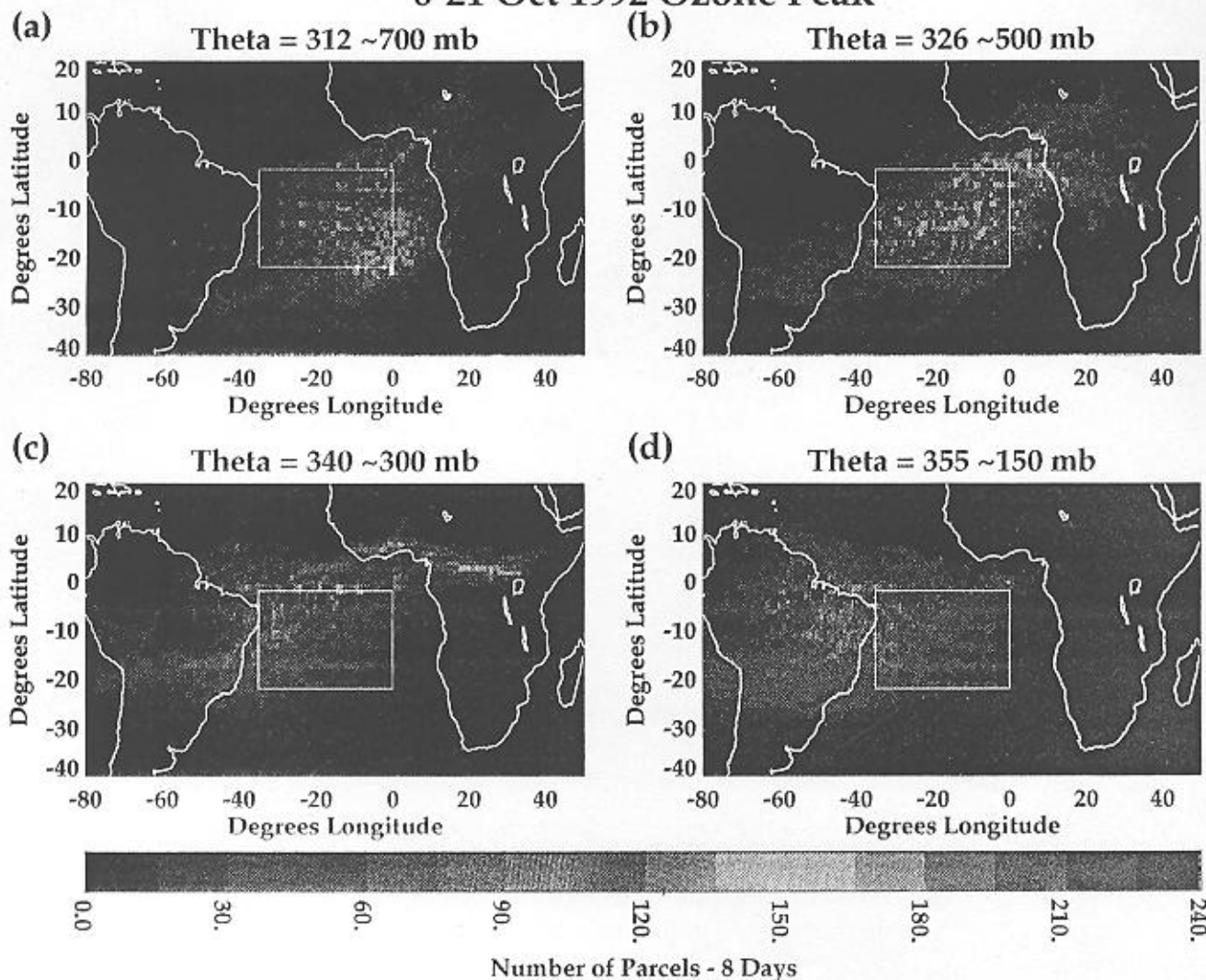


**Plate 2.** Hourly parcel locations along 8-day backward trajectories from region of maximum tropospheric  $O_3$  column (box) identified from map in Plate 1. Four levels shown, approximately (a) 700 mbar, (b) 500 mbar, (c) 300 mbar, (d) 150 mbar. Higher-altitude  $O_3$  supplied by Brazil and possibly central Africa where deep convection supplies  $O_3$  precursors to upper troposphere.

ozone distributions in 5-km increments (thickness in Dobson units) for all sounding sites in Figure 1 except La Réunion. "Background  $O_3$ " amounts for Ascension, Brazzaville, Natal, and Irene are computed by averaging over all the individual profiles (recorded in 1-km increments) in March–April–May 1990–1992. These are the months of lowest-fire activity and correspond to the annual minimum in tropospheric ozone [Thompson *et al.*, this issue]. Adding of the columns from 0–15 km for each site gives "background" column depth from 26 to 32 DU. This supports the choice of 26 DU for nonpolluted tropospheric column depth over eastern equatorial Africa and the Indian Ocean in the TOMS map (Plate 1). In Table 4 "excess ozone" in each layer is derived by subtracting the background mean profile for each site from the profiles measured during September and October 1992 and averaging over this set.

Back trajectory initializations correspond roughly to the midpoints of the layers in Table 4. For each day on which a

sounding was made between September 15 and October 24, 1992, 8-day isentropic back trajectories (in clusters) were initialized from the lower ( $\sim 3.5$  km), middle ( $\sim 7.5$  km), and upper ( $\sim 12.5$  km) troposphere using ECMWF winds. Origin points for individual trajectories (eight days earlier) sorted according to direction from the sounding locations are shown in Figure 8. Although this summary covers a longer period than the satellite TOMS-fire count analysis (six weeks versus 15 days in Plate 2), a similar picture emerges. Namely, Ascension Island ( $8^\circ S$ ,  $14^\circ W$ , in the middle top third of the Plate 2 box) and Natal (western edge of the box) could be supplied with  $O_3$  and/or  $O_3$  precursors from South America above 300 mbar following deep convection. At midtropospheric level, Ascension, Natal, and Brazzaville have air parcel origins predominantly ( $>60\%$ ) from the east (Figure 8) with travel over Africa from  $5^\circ N$  to  $20^\circ S$ . Examination of representative soundings and trajectories at Ascension, Brazzaville, and Natal gives more insight into these processes.

## Forward Trajectories From Fires, Oct 1-15, 1992

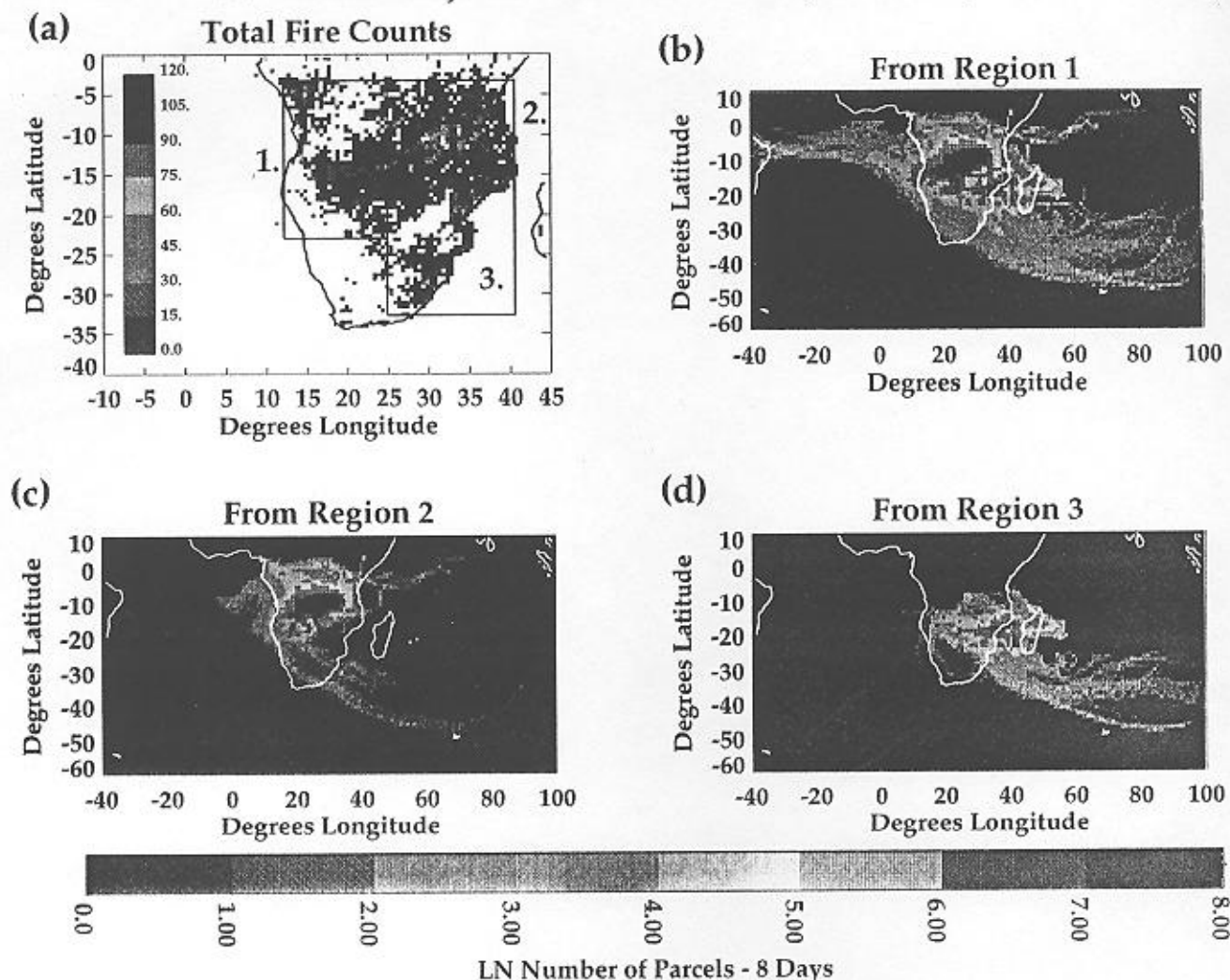


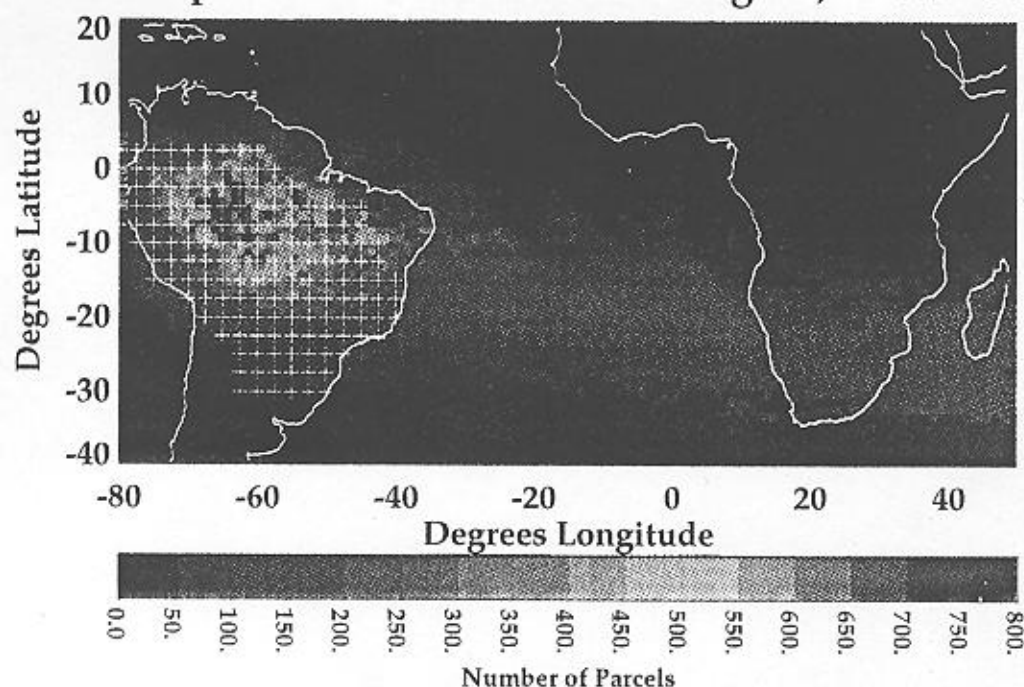
**Plate 3.** Parcel (hourly) locations from forward trajectories (8 days) run with isentropic model and ECMWF analyzed winds from (a) fires in regions (b) 1, (c) 2, and (d) 3 during October 1–15, 1992. LN is natural log. Eight-day trajectories initialized each day for which there are fire counts (missing days October 2, 6, 8, 10). Clusters initialized in proportion to fire counts. Recirculating, very slow parcels lead to the composite with high density of parcels over southern Africa.

**Ascension, Brazzaville, and Natal.** Two examples of Ascension soundings with ozone column depth  $>60$  DU appear in Figure 9. Prominent  $O_3$  maxima in the 10- to 15-km layer correspond to direct flow from biomass burning regions with deep convection in northeastern Brazil. Day 271 (September 27, 1992) is the date of DC-8 sampling of convective outflow over Brazil (flight 6) [see Pickering *et al.*, this issue (a)]. For 14 of 17 Ascension soundings between September 15 and October 24, 1992, the origin of upper tropospheric air parcels was eastern South America with transit times usually less than 4 days. The September 27 sounding corresponds to trajectories with more concentrated origin (tighter clusters) than the October 9 sounding. Both soundings show the  $\sim 3.5$ -km back trajectory originating in Africa, which is typical ( $>90\%$  from east in Figure 8a), but midtropospheric origins differ. On September 27 the origin at  $\sim 7$  km was Africa and on October 9 it was Brazil (Figure 9b). In both cases, integrated tropospheric  $O_3$  from 5 to 10 km was 22–23 DU, 10 DU more than for the background amount at Ascension (Table 4).

At Natal, along the Brazilian coast, upper tropospheric origins were South America for all 15 soundings between September 15 and October 24, 1992. This explains the 100% western origin in Figure 8c. Thin layers of high  $O_3$  at what are presumed to be cloud outflow levels are shown in Figure 10a. Forward trajectories from the large convective system sampled on September 27 (flight 6) showed transit toward Natal (Figure 10b). From September 28 to 30, increases throughout middle and upper troposphere result in an increase in integrated tropospheric  $O_3$  (0–15 km) from 54 to 61 DU. Back trajectories corresponding to the 12.5-km layers at Natal originate from interior Brazil [Pickering *et al.*, this issue (a)]. However, middle and lower troposphere back trajectories show direct flows from the Atlantic (very slow, not reaching Africa in  $>1$  week) and/or Africa from outflow regions along the Gulf of Guinea coast (Figure 10c).

Forward trajectories from the Flight 6 convective region suggest  $\sim 1$  week transit time to Ascension Island. Elevated  $O_3$  at 10–15 km, where increases at Natal were pronounced, ap-

a) **Forward Trajectory Parcel Distribution**  
 25 Sep-20 Oct 1992 Convective Region, Theta= 340



b) **Forward Trajectory Parcel Distribution**  
 25 Sep-20 Oct 1992 Convective Region, Theta= 340

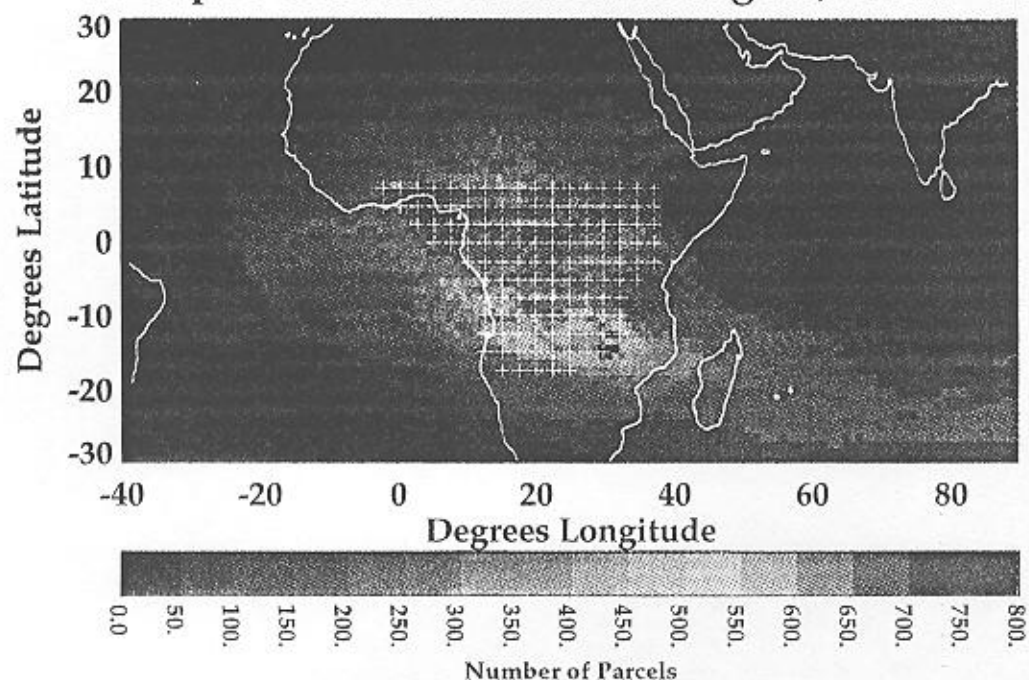


**Plate 4.** Parcel locations (hourly) determined from forward trajectories (8 days) run with isentropic model and ECMWF analyzed winds from (a) region in Brazil with biomass fires and deep convection in late September through October 20, 1992. (b) Same for Africa. Starting level is approximately 10 km, determined by average cloud-top pressure of ISCCP deep convective clouds for September and October 1992.

**Table 4.** Seasonal Tropospheric Ozone Anomaly, September–October 1992 Versus March–April–May Means (1990–1992)

Site	0–5 km Layer		5–10 km Layer		10–15 km Layer	
	Background O <sub>3</sub> , DU	Excess O <sub>3</sub> , DU	Background O <sub>3</sub> , DU	Excess O <sub>3</sub> , DU	Background O <sub>3</sub> , DU	Excess O <sub>3</sub> , DU
Ascension	11.6	9.3	11.4	6.3	6.6	3.4
Brazzaville	12.1	4.5	11.8	3.2	8.1	3.1
Natal	12.1	7.7	11.6	5.7	7.8	3.2
Okaukuejo	9.7	4.8	11.0	3.8	7.2	2.5
Irene	8.1	3.3	10.7	4.1	8.8	1.9

Okaukuejo background profile from Réunion, Brazzaville, Ascension mean.

pears in the 3 and 5 October 1992 soundings, which back trajectories show originated over South America (Figure 11). Excess O<sub>3</sub> (relative to a March to May Ascension reference) is 4 DU for these soundings.

In general, Ascension and Natal tropospheric O<sub>3</sub> columns during SAFARI/TRACE A are larger than at Brazzaville (Figure 3, Table 4). Only one Brazzaville sounding showed parcels

with a Brazilian origin and 6 of 11 soundings showed upper tropospheric trajectories with little (1 DU) or no excess O<sub>3</sub>. Some of this resulted from sampling time and frequency; of the 11 soundings, only 3 were taken in September. The relatively low upper tropospheric O<sub>3</sub> in October corresponded to recirculation over Africa, toward the northern hemisphere or to the east where burning had tapered off (Figure 7). The lowest

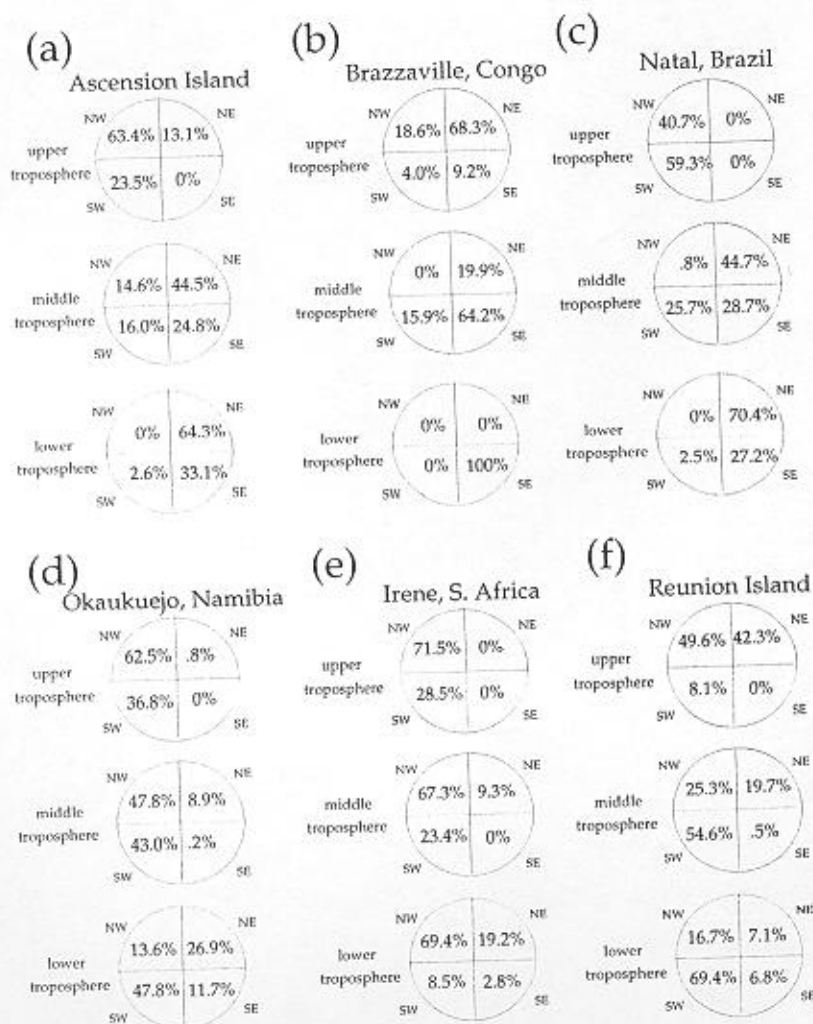


**Figure 8.** Summary of 8-day back trajectories initiated from three levels at each sounding site on days of ozonesonde launch. A cluster of 121 points is centered at the location of each site at starting potential temperature surfaces corresponding to points at  $\sim 3.5$  km ( $\theta = 350$  K, "lower troposphere"),  $\sim 7.5$  km ("middle troposphere"), and 11–12 km ("upper troposphere"). Origin points, categorized by quadrant relative to sounding site, are summed over number of days of soundings to derive percentages: (a) Ascension, (b) Brazzaville, (c) Natal, (d) Okaukuejo, (e) Irene, (f) Réunion.

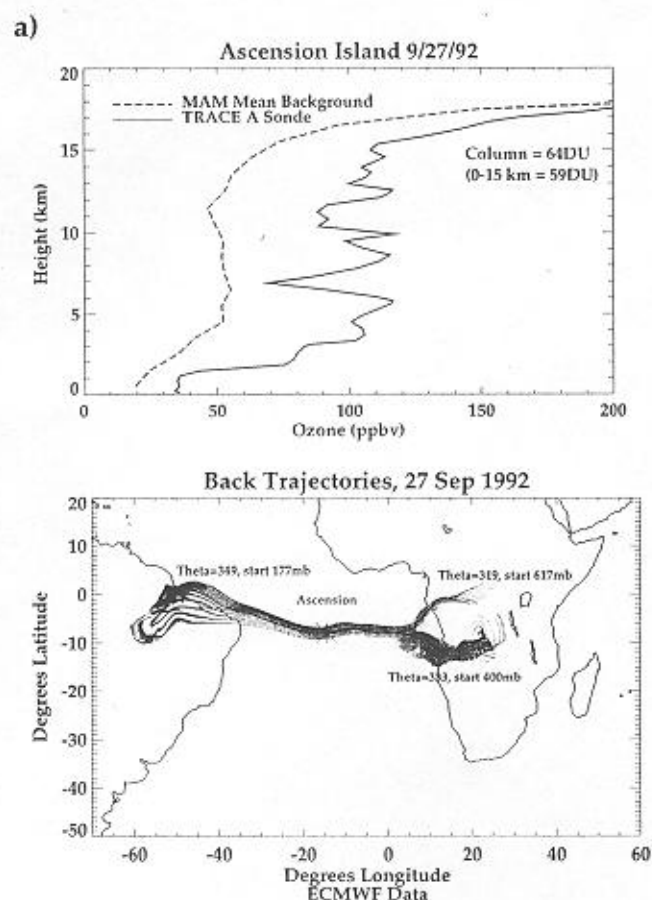


**Figure 9.** Ozone profiles and corresponding trajectories at upper (~11.5 km), middle (~7.5 km), and lower (~4 km) tropospheric levels from two Ascension Island soundings. M-A-M background (dashed lines in soundings) refers to mean profile from sondes in March–April–May during 1991–1992; this is time of year for which biomass burning is a minimum. (a) Day 271, September 27, 1992; (b) day 283, October 9, 1992. Total integrated tropospheric ozone was 64 DU on September 27, and 62 DU on October 9, the highest  $O_3$  column depths during SAFARI/TRACE A (Figure 3a).

Brazzaville tropospheric  $O_3$  (Figure 3, days 291 and 293) coincided with back trajectories that were tightly clustered E/NE toward Kenya and Tanzania. During this time, TOMS-derived tropospheric  $O_3$  shows low-ozone column (30 DU) for eastern Equatorial Africa (Plate 1) and AVHRR imagery shows extensive cloud cover). The day 291 and 293 samples bias the mean tropospheric  $O_3$  statistics in Table 4. If they are omitted, average column  $O_3$  (0–15 km) at Brazzaville would be 49 DU instead of 46 DU.

There were seven days with soundings at both Ascension and Brazzaville, and Brazzaville tropospheric  $O_3$  was 4–25 DU lower than Ascension for five of them (Figure 3). These five days corresponded to African and/or Atlantic air mass origin below 10 km for both sites. Why are  $O_3$  concentrations higher at Ascension? A decrease in fire sources, closer to Brazzaville than to Ascension, has already been mentioned. Although  $O_3$  formation rates near fires are substantial (4 DU/d below 4 km, section 4) and Brazzaville is nearer sources than Ascension,  $O_3$  destruction over the continent is much faster than in the marine boundary layer. Besides diurnal mixing, shallow and deep

convection can mix  $O_3$ -rich layers toward surface removal. These processes were active in early and mid-October near Brazzaville, according to cloud imagery and TOMS reflectivity (note gap in  $O_3$  map, Plate 1). In contrast,  $O_3$  in the free troposphere, in transit from Africa to Ascension, has a 2–3 week lifetime (Table 5) [see also Jacob *et al.*, this issue].

Further insight into differences between Ascension and Brazzaville comes from considering the soundings on October 18, 1992 (Figure 12). The Ascension sounding shows a 12-km maximum ( $O_3$  mixing ratio >120 ppbv) in an air parcel with less than 2 days' transit time from Brazil, whereas maxima (layers >80 ppbv) from 5 to 7 km are associated with recirculated Atlantic air parcels just west of Angolan burning regions. Ozone was measured on TRACE A flight 15 (Figure 1) on the same day, E/SE of Ascension. Ozone sampling from the DC-8 showed maxima with mixing ratios similar to the Ascension soundings at the same altitudes (Figure 16, below) and back trajectories from the aircraft locations showed South American (from 12 km) and African (from 5–10 km) origins. Throughout most of flight 15, NO concentrations were 100–300 pptv, which supports 1–2 DU/d ozone formation in the upper troposphere. Thus a second reason for higher  $O_3$  at Ascension is residual  $O_3$  formation in the middle and upper troposphere, as observed over the Atlantic. A third reason appears to be widespread subsidence over the Ascension area [Krishnamurti *et al.*, this issue], which is manifest in persistent marine stratocumulus and the discontinuity in the  $O_3$  profile at Ascension (Figures 11, 12a). The latter is at 1.5 km; compare  $O_3$  profiles during DC-8 ascents and descents through the marine stratocumulus

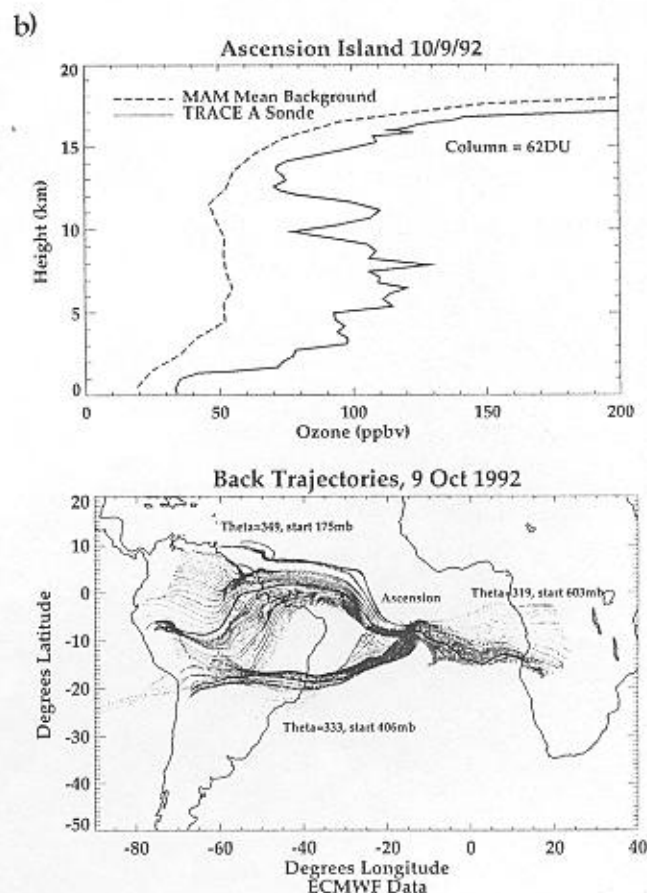


**Figure 9.** (continued)

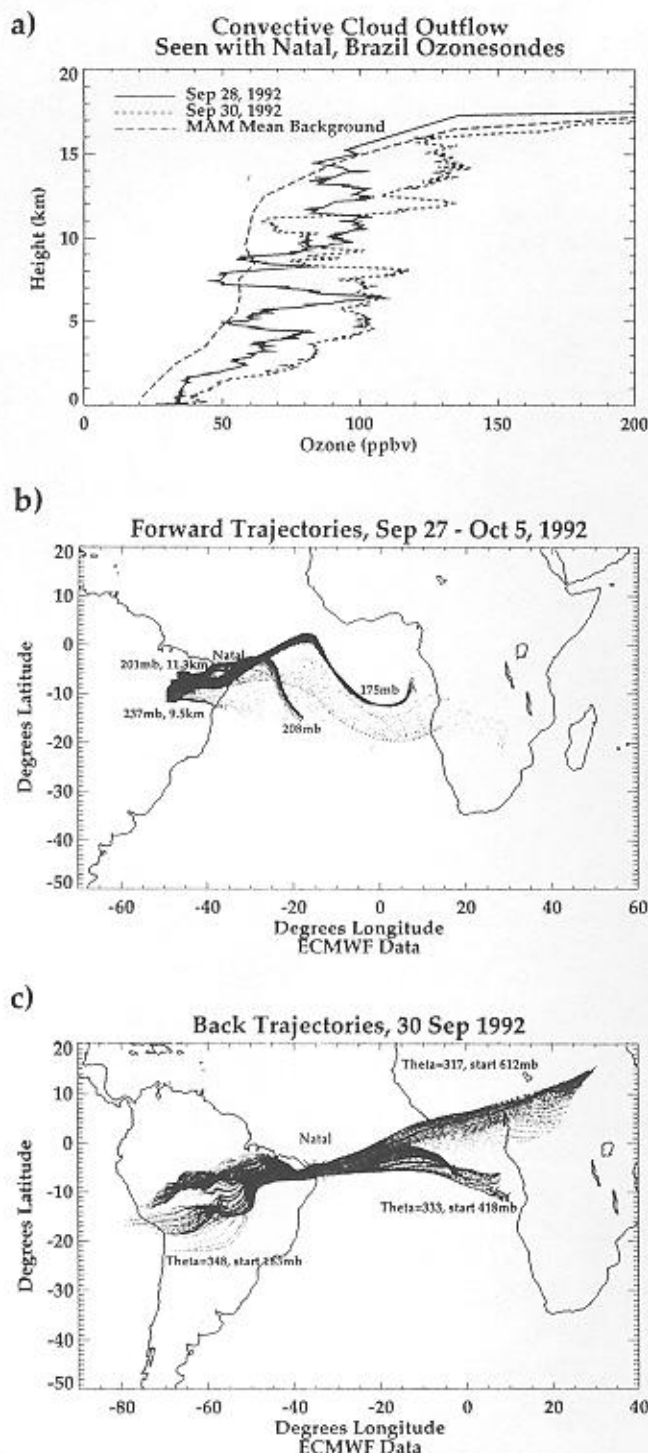
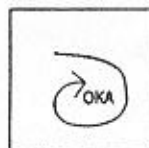


**Figure 10.** (a) Ozone profiles from Natal, Brazil, soundings on September 28 and 30, 1992. Impact of deep convection apparent with enrichment of 10–15 km ozone. M-A-M background (dashed line) refers to mean profile from Natal sondes in March–April–May of 1991–1992. (b) Forward trajectories from flight 6 at cloud outflow levels head toward Natal and Ascension Island. (c) Back trajectories at ~12.5 km (183 mbar) from September 30 sounding show origin in convectively active region with biomass fires. Lower-level O<sub>3</sub> originates from Africa. Start points are 418 mbar (7 km) and 612 mbar (4 km).

[Gregory *et al.*, this issue]. The O<sub>3</sub> photochemical lifetime at 8–12 km is >1 month (Table 5) and steady subsidence to middle and lower troposphere can enrich profiles at Ascension and Natal. Sampling off Natal on the NASA Electra in October 1989 detected aged biomass burning O<sub>3</sub> layers from Africa and South America [Andreae *et al.*, 1994b].

Figure 10 (September 30, 1992) is another example of mixed O<sub>3</sub> origins at Natal. Although the 5- to 9-km layer is >100 ppbv, the corresponding trajectories are more than a week removed from Africa (Figure 10c). For the 16 Natal O<sub>3</sub> soundings between September 15 and October 24, 1992, nearly all middle- and lower-level trajectory clusters had Atlantic and/or African origin, with only a few parcels originating from South America. Thus Natal, like Ascension, is enriched at low levels by slowly moving air parcels with long-lived O<sub>3</sub> of African origin, a mechanism first suggested by Logan and Kirchhoff [1986]. The mean flow of total O<sub>3</sub> seen in the Hovmöller plots (Figure 6), easterlies dominating between 0° and 10°S, is consistent with back trajectories from Natal and Ascension soundings during SAFARI/TRACE A.

**Okaukuejo, Réunion, and Irene.** Compared to tropical sites (Ascension, Natal, and Brazzaville), the origins of the three sites between 20° and 26°S are more complex. This is implied in the trajectory climatologies (Plates 2–4) as well as in the origins of the soundings summarized in Figure 8. Note that the categorization can be misleading in some cases of recirculation, and travel distances from origin to arrival point are not indicated in Figure 8. The following pattern, for example, would be labeled NW for a back trajectory arriving at Okaukuejo although biomass fire exposure was Zambia to the NE:



The Irene sounding with highest tropospheric O<sub>3</sub> during SAFARI/TRACE A appears in Figure 13. In this case, upper tropospheric flow was more likely from the Pacific or the urban coast of South America than from savanna burning regions. Upper tropospheric O<sub>3</sub> enrichment at Okaukuejo also correlates well with rapid transit from South America. Note the predominance of NW origins in the upper troposphere (Figure 8d). Diab *et al.* [this issue (b)] noted that Okaukuejo soundings at lower altitudes fell into two categories depending on the synoptic situation. Extensive anticyclonic recirculation over Africa and the eastern Atlantic [Garstang *et al.*, this issue] was often manifested in high ozone (>50 ppbv) throughout the middle and lower troposphere. Westerly troughs brought in marine air above the mixed layer, leading to a localized minimum. Figure 14 shows Okaukuejo profiles for October 10 and 11, with the trajectories at ~7.5 km signaling a marked transition in air mass origin; on October 11 (day 285) the midlevel flow to Okaukuejo is from the SW and largely marine. Other days on which the westerly trough dominated at Okaukuejo were September 27 and October 13 and 14, 1992; tropospheric O<sub>3</sub> to 15 km was <35 DU on those days.

Réunion is just south of 20°S and only five soundings were taken during SAFARI/TRACE A (Figure 5e). Integrated tropospheric column O<sub>3</sub> reached 50 DU or more twice during this period (Figure 3b). Baldy *et al.* [this issue] describe general

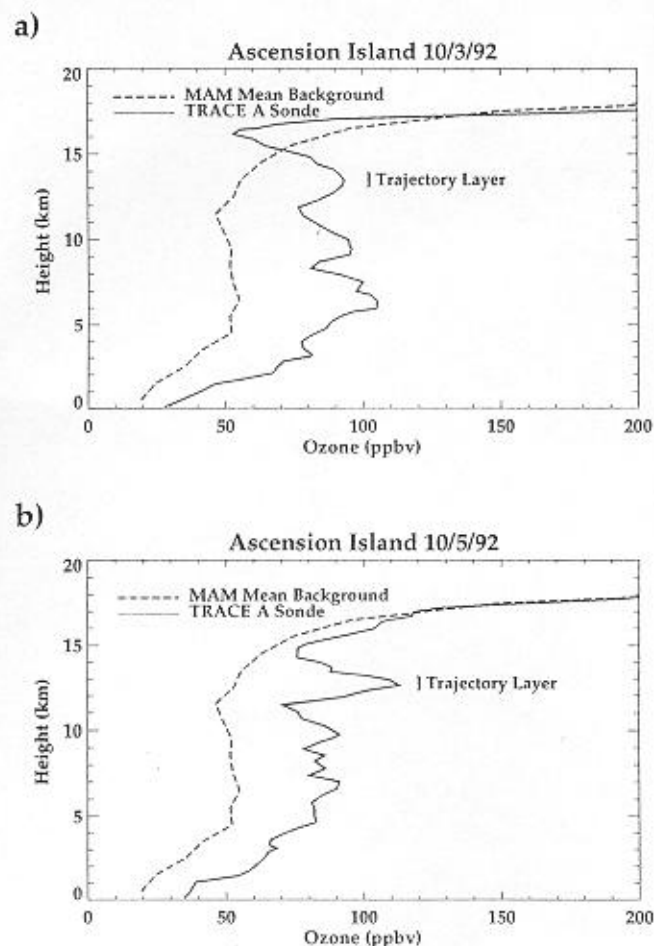


**Figure 11.** (a) Ozone profiles at Ascension Island, downwind of Brazilian biomass burning and convection on (a) October 3 and (b) October 5, 1992. M-A-M background (dashed line) refers to mean profile from Ascension sondes in March–April–May during 1991–1992. Back trajectories at (c and d)  $\sim 11.5$  km are indicated.

features of these soundings. At low and middle level, Réunion back trajectories are predominantly from the west (Figure 8f), with air parcels that passed over fires in east Africa highest in  $O_3$ . Note that Mozambique fires are frequently upwind of Réunion (Plate 3d). Using tracers measured on the Indian Ocean TRACE A flight 11 (October 9, 1992), Gregory *et al.* [this issue] present evidence to support an African source for elevated ozone in that region. A flight profile due east of Mozambique, with several days' transit from the SW African coast and Madagascar, showed concentrations of  $O_3$  precursors ( $CO$ ,  $C_2H_6$ , and  $C_3H_8$ ) twice as high as for a flight 11 profile southeast of the African coast which 5-day back trajectories place as remote marine in origin.

Upper tropospheric  $O_3$  in the Réunion soundings appears to correspond to cloud outflow levels from Africa and South America (Plate 4). Some trajectories that passed over African burning areas were recirculated from the Indian Ocean and appear as NE in Figure 8f.

#### 4. "Where Did the Ozone Come From?": Role of Photochemistry

The Hovmöller plot for the tropical band (Figure 6a) can be used to estimate a photochemical formation rate for ozone

during TRACE A. Assume that the Atlantic-African gradient in free tropospheric  $O_3$  is represented by the mean Ascension-Brazzaville difference in column ozone. This is 6.9 DU (mean tropospheric  $O_3$  at Ascension is equal to 52.5 DU in September–October 1992 and at Brazzaville is equal to 45.6 DU). Slopes of  $O_3$  maxima in the Hovmöller plot are equivalent to a 4- to 7-day rate of  $O_3$  propagation from Brazzaville ( $15^\circ E$ ) to Ascension ( $14^\circ W$ ). Thus if Ascension (Atlantic) has tropospheric  $O_3$  7 DU greater than Brazzaville (Africa), there is an implied net  $O_3$  formation over the Atlantic of 1–1.4 DU/d (equivalent to several ppbv  $O_3$ /d in the free troposphere). This rate of free tropospheric  $O_3$  photochemical formation is consistent with instantaneous point modeling of aircraft data from free tropospheric TRACE A sampling over the Atlantic from  $0^\circ$  to  $20^\circ S$ , e.g., flights 13–17 [Jacob *et al.*, this issue] (section 4.1). Larger rates of  $O_3$  formation are computed from the major TRACE A source characterization flight over southern Africa (flight 10) and from SAFARI DC-3 observations [Thompson *et al.*, 1996; Zenker *et al.*, 1996]. In the following sections, point modeling of ozone from several of these flights is described.

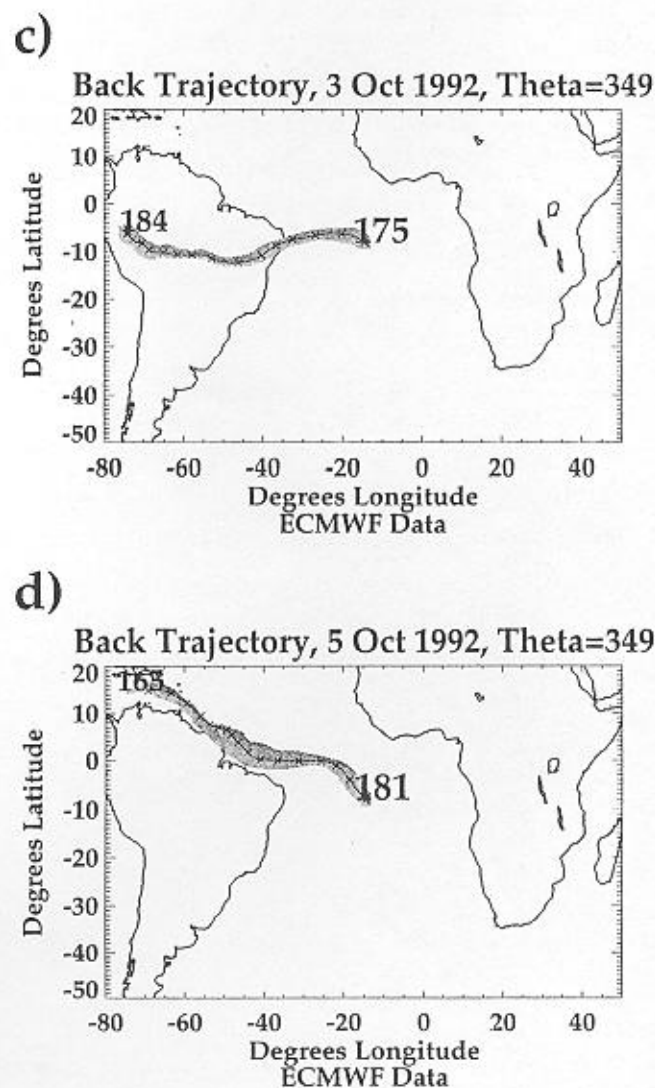


**Figure 11** (continued)



**Table 5.** Ozone Production and Loss Characteristics of Air Masses Sampled on TRACE A DC-8 Flights 6 and 10-17

	TRACE A Flight							
	10	12	13	14	15	16	17	6 <sup>a</sup>
Mean O <sub>3</sub> , 0-4 km (ppbv)	70	68	51	50	57	61	58	46
P-L in ppbv/d, 0-4 km	14	-1.8	-5.6	-6	-2.6	-4.3	-3.3	4.8
P-L in DU/d 0-4 km	3.9	-0.49	-1.6	-1.7	-0.74	-1.2	-0.89	1.4
Tau, O <sub>3</sub> = [O <sub>3</sub> ]/loss rate, 0-4 km	7.9	8.0	4.6	4.6	7.7	7.5	7.5	5.0
RT, O <sub>3</sub> = [O <sub>3</sub> ]/prod. rate, 0-4 km	3.3	10	9.5	10	12	16	13	3.6
Mean O <sub>3</sub> , 4-8 km (ppbv)	84	64	59	61	68	75	85	71
P-L in ppbv/d, 4-8 km	0.36	-3.3	-0.57	-0.04	1.6	-0.11	0.49	-0.18
P-L in DU/d, 4-8 km	0.07	-0.74	-0.11	-0.01	0.26	-0.02	0.09	-0.03
Tau, O <sub>3</sub> = [O <sub>3</sub> ]/loss rate, 4-8 km	29	9.1	13	19	46	21	25	16
RT, O <sub>3</sub> = [O <sub>3</sub> ]/prod. rate, 4-8 km	26	17	15	19	22	22	22	17
Mean O <sub>3</sub> , 8-12 km (ppbv)	81	na	78	67	61	82	73	76
P-L in ppbv/d, 8-12 km	1.6	na	2.6	2.5	1.8	1.5	2.2	2.1
P-L in DU/d, 8-12 km	0.23	na	0.32	0.29	0.22	0.17	0.24	0.26
Tau, O <sub>3</sub> = [O <sub>3</sub> ]/loss rate, 8-12 km	32	na	121	122	160	218	179	94
RT, O <sub>3</sub> = [O <sub>3</sub> ]/prod. rate, 8-12 km	20	na	25	22	28	44	28	27
Mean O <sub>3</sub> , 0-12 km (ppbv)	75	66	61	60	61	80	70	60
P-L in ppbv/d, 0-12 km	8.6	-2.6	-2.0	-1.1	1.1	0.99	-0.32	2.7
P-L in DU/d, 0-12 km	6.2	-1.9	-1.3	-0.67	0.49	0.40	-0.18	1.9
Tau, O <sub>3</sub> = [O <sub>3</sub> ]/loss rate, 0-12 km	12	8.5	9.6	12	37	66	18	9.7
RT, O <sub>3</sub> = [O <sub>3</sub> ]/prod. rate, 0-12 km	5.4	13	14	16	23	37	19	7.2

<sup>a</sup>Flight 6, Brasilia local, September 27, 1992. P-L, O<sub>3</sub> in 8-12 km layers corresponding to cloud outflow are 6-7 ppbv O<sub>3</sub>/d [Pickering *et al.*, this issue (a)].

<sup>b</sup>Tau, O<sub>3</sub> lifetime, in days.

<sup>c</sup>RT, replacement time, days.

#### 4.1. Photochemical "Point" Modeling of Source Regions

Jacob *et al.* [this issue] cover photochemical point (instantaneous steady state) modeling for TRACE-A flights 4-17 in detail. They give an overview of ozone formation and selected comparisons of computed and observed species concentrations using the Harvard tropospheric chemistry scheme. Heikes *et al.* [this issue] use the Harvard point model and GSFC one-dimensional model to describe tropical marine boundary layer chemistry on selected TRACE A flights. The GSFC point model is in good agreement with the Harvard model (A. M. Thompson *et al.*, unpublished manuscript, 1996), so we present computations only for prototype flights 6, 10, and 15.

The photochemical scheme used in the GSFC point model [Thompson, 1996] has 128 photochemical reactions describing transformations among 38 species. Besides chemistry based on standard odd oxygen, odd hydrogen, odd nitrogen, CH<sub>3</sub> and C<sub>2</sub>H<sub>6</sub> reactions, representative nonmethane hydrocarbons (propane, propene, ethene, and toluene), and by-products of their oxidation are specified. Photolysis inputs are based on TOMS-derived overhead ozone measured during TRACE A, and October 1, 1992, solar input is assumed. The point model computes transients and nonmeasured constituents with the model constrained by mixing ratios of O<sub>3</sub>, CO, NO, hydrocarbons, H<sub>2</sub>O, UV flux, and temperature measured at 180-s (or greater) intervals on the DC-8. Computed transient species concentrations (O(<sup>1</sup>D), HO<sub>2</sub>, R<sub>i</sub>O<sub>2</sub>) are used to evaluate net O<sub>3</sub> formation from

$$\begin{aligned}
 P - L(O_3) = & k_1[NO][HO_2] + \sum k_i[NO][R_iO_2] \\
 & - [O_3]\{k_3[OH] + k_4[HO_2]\} \\
 & - k_5[O(^1D)][H_2O],
 \end{aligned}$$

where R<sub>i</sub>O<sub>2</sub>, organic peroxy radicals, include CH<sub>3</sub>O<sub>2</sub>, C<sub>2</sub>H<sub>5</sub>O<sub>2</sub>, C<sub>3</sub>H<sub>7</sub>OHO<sub>2</sub>, C<sub>2</sub>H<sub>4</sub>OHO<sub>2</sub>, C<sub>3</sub>H<sub>7</sub>OHO<sub>2</sub> (both *n*- and *i*), and CH<sub>3</sub>CO<sub>2</sub>.

The primary TRACE A sampling in active fire regions was on flight 10 (Figure 1), which took place on October 6, 1992, during a flight from Johannesburg to northern Zambia (fire-rich region at 10°S, 30°E in Figure 7). Figure 15 shows O<sub>3</sub>, NO, CO, and one hydrocarbon (propane) from that flight. The O<sub>3</sub> mixing ratio is high (80-110 ppbv) on the two brief flight segments in haze layers (1040 and 1200 UT), but similar concentrations were recorded at ~6 km (1230 UT) and on the 10-km leg. Not all the highest NO readings were in the haze layer. Values of 200-400 pptv NO at 10 km (Figure 15c) do not coincide with elevated NO<sub>y</sub>, except at one point and do not correlate with elevated hydrocarbons, CO, PAN or HNO<sub>3</sub>; lightning is a possibility. Figure 15e shows net O<sub>3</sub> production calculated with the GSFC point model. Low-altitude legs, corresponding to sampling in northern Zambia, show equivalent net formation rate 14 ppbv O<sub>3</sub>/d (4 DU/d integrated from 0 to 4 km). For 4-8 km the rate falls off (0.4 ppbv/d), but in the upper troposphere (layer defined as 8-12 km), the rate is equivalent to 1.6 ppbv O<sub>3</sub>/d.

The upper troposphere O<sub>3</sub> formation rate computed for flight 10 is typical of all TRACE A flights [Jacob *et al.*, this issue] (Table 5). Conditions of temperature, UV and sufficient concentrations of NO appear to make the tropical upper troposphere a region of O<sub>3</sub> and OH formation. Table 5 shows that on average over flight 10, O<sub>3</sub> formation is 9 ppbv/d (equivalent to 6 DU O<sub>3</sub> formation/d). The average calculated lifetime is 8 days in the boundary layer and ~30 days in the middle and upper troposphere (Table 5). Overturning of upper tropospheric air suggests that a more realistic lifetime is 2-3 weeks.

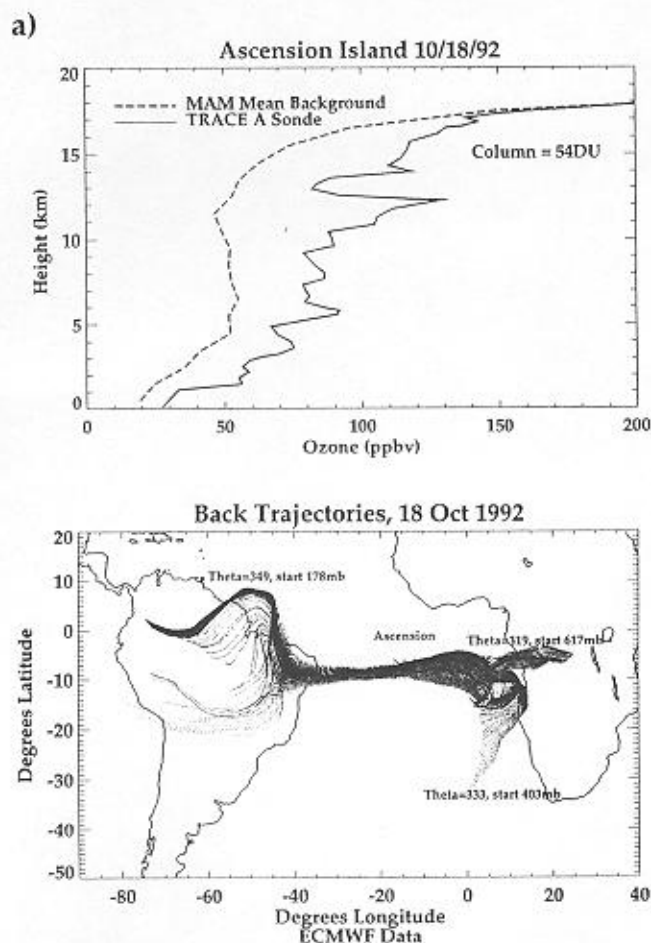


**Figure 12.** Soundings at (a) Ascension and (b) Brazzaville, along with back trajectories, for day 292, October 18, 1992. M-A-M background (dashed lines) refers to mean profile from sondes at each site in March–April–May during 1991–1992. Starting levels are approximately 12.5 km (178, 187 mbar), 7 km (403, 417 mbar), and 4 km (617, 625 mbar). Compare in situ sampling in eastern Atlantic on flight 15, Figure 16.

Flight 10 was the only African TRACE A flight with sustained sampling in a region with extensive active and recent biomass burning. We also performed point modeling with a set of 60 points from SAFARI DC-3 flights (shaded region in Figure 1), over a range of regimes at less than 4 km [Thompson *et al.*, 1996; Zenker *et al.*, 1996]. Simulations were performed for three separate flights on September 26 and 27 and October 1, 1992. These flights sampled typical background air for southern Africa, with  $O_3$  mixing ratios ranging from 40 to 75 ppbv. In the flight segment near Victoria Falls, where the highest  $O_3$  concentrations were encountered by the DC-3, net  $O_3$  production was equivalent to 11 ppbv  $O_3/d$ . Rates of ozone formation from the DC-3 samples averaged 20–25% less than those for the DC-8 flight 10 boundary layer samples. Thus the SAFARI and TRACE A data sets appear to give a consistent picture of ozone formation and suggest that the flight 10 analysis typifies ozone formation over southern African savanna burning regions from 10° to 20°S during late September to early October 1992.

#### 4.2. Point Modeling of TRACE A African Outflow Flights 13–17

Table 5 gives net  $O_3$  production rates for the Atlantic outflow flights from Windhoek (TRACE A flights 13–16) and for

the Ascension local flight 17 (October 22, 1992). Net  $O_3$  formation is uniformly positive above 8 km because NO mixing ratios >100 pptv are typical,  $H_2O$  is low ( $H_2O$  destroys  $O_3$  via reaction between  $O(^1D)$  and  $H_2O$ ), and CO (which converts OH to  $HO_2$ , leading to  $O_3$  formation) tends to be elevated over background (100 or more ppbv versus 60–80 ppbv at background). Figure 16 illustrates the Atlantic regime with DC-8  $O_3$ , NO, and CO data from flight 15 (October 18, 1992, day 292). Back trajectories from two of the flight 15  $O_3$ /NO/CO maxima (Figure 16e) show origins in Africa (at 1130 UT, 10-km leg) and South America (1500 UT at 12 km). This is similar to origins of middle and upper tropospheric ozone from the October 18 sounding at Ascension (Figure 12a), not far from flight 15 sampling (Figure 1). However, the 10- to 12-km layer at Brazzaville on October 18 appears to be from Africa (Figure 12b), where persistent convection at 0°–15°S is seen in AVHRR imagery. Trajectories from levels corresponding to the Brazzaville  $O_3$  maximum above 15 km (not shown) also point to Africa origins. Net photochemical  $O_3$  formation on flight 15 (Figure 16d) is 1.8 ppbv  $O_3/d$  at 8–12 km (equivalent to 0.2 DU/d). With transit times of 4–7 days from fires or from deep convection, a parcel traveling to the Atlantic could accumulate several DU in the 8- to 12-km level. Therefore higher  $O_3$  columns, at least above the mixed layer, are expected downwind from sources rather than in the vicinity. Through the entire tropospheric column (0–12 km)  $O_3$  formation is 0.5 DU/d, half the rate deduced from the Hovmöller diagram at

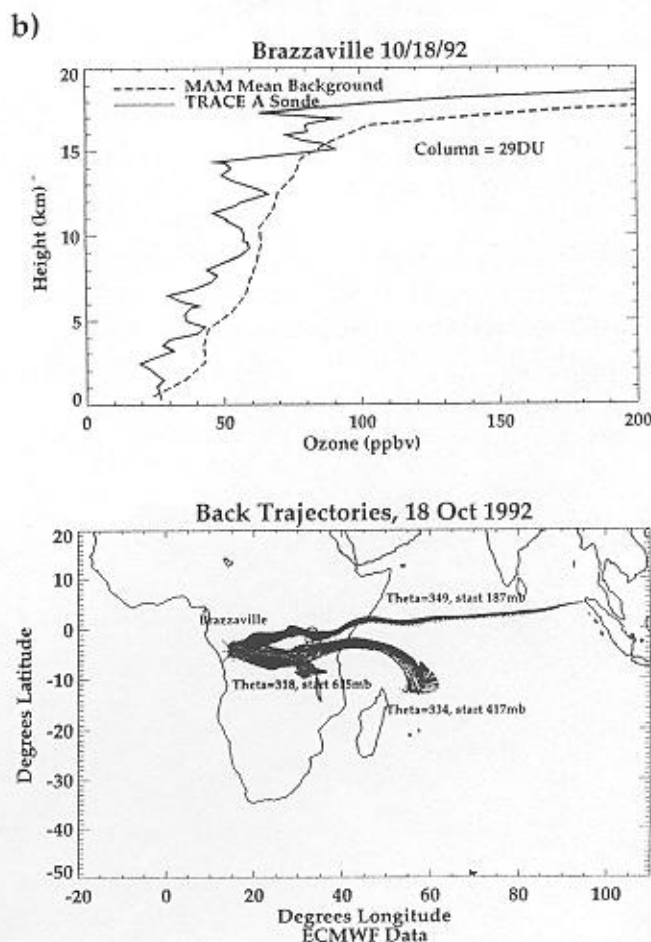


**Figure 12.** (continued)

0°–10°S. Gregory *et al.* [this issue] present a comparison between profiles taken on African outflow flights 15 (October 18, 1992) and 13 (October 14), approximately 1000 km and 2 days transport time to the east. Ozone precursors in the lower midtroposphere, e.g., CO and hydrocarbons, are 30% reduced in the additional transit time from the continent, and the ozone column to 7 km has increased 4.5 DU. This rate of O<sub>3</sub> formation is greater than implied by our model calculations of flight 13–15 data. Inasmuch as virtually all TRACE A sampling implied NO<sub>x</sub>-limited ozone formation, the rates suggested by Gregory *et al.* [this issue] appear to require more NO than we used in the point model (3-min averages from the Harvard merged data set). This could mean an in situ NO source, perhaps lightning upwind of sampling.

The apparent cause of CO/NO<sub>x</sub>/hydrocarbon enrichment in the upper troposphere is advection following convection from regions with elevated O<sub>3</sub> or O<sub>3</sub> precursor concentrations. Interpretations of tracers and reactive nitrogen partitioning on the Atlantic TRACE A flights [Gregory *et al.*, this issue; Jacob *et al.*, this issue; Smyth *et al.*, this issue; Singh *et al.*, this issue; C96] argue for a significant lightning NO source. Flight 6 (section 4.2 below) also provided strong evidence for the lightning source, directly in cloud-outflow NO sampling and, indi-

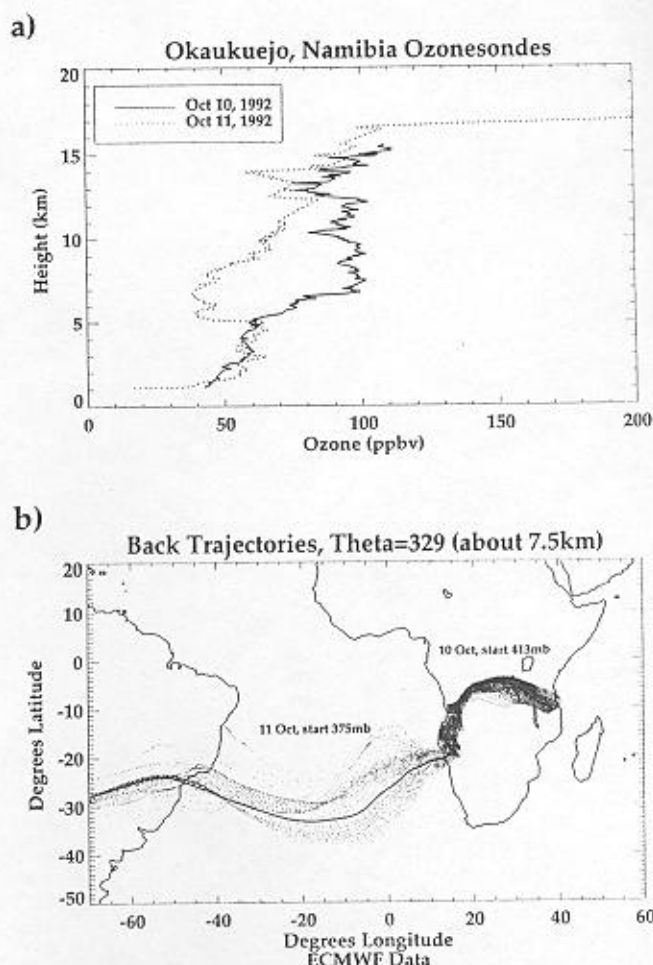


Figure 14. Transition from an anticyclone regime (October 10, 1992) to westerly trough (October 11, 1992) as seen in Okaukuejo O<sub>3</sub> soundings. (b) Midlevel back trajectories (~7.5 km) from GSFC isentropic model show flow transition with westerly, marine origins for the October 11, 1992, sounding.

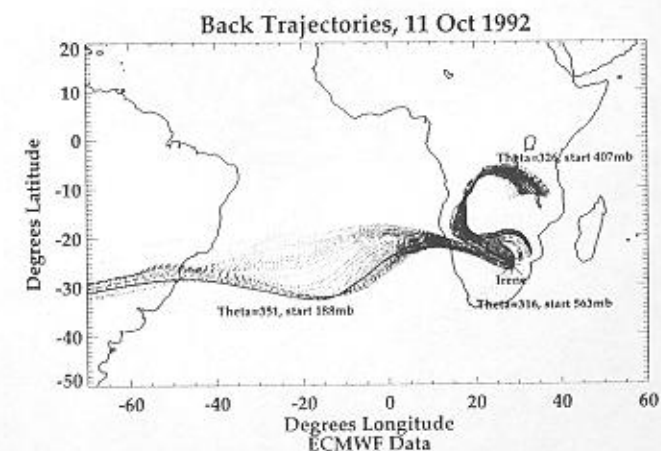
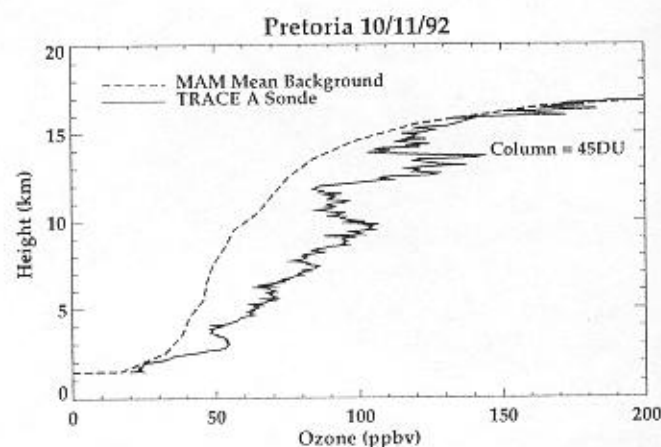
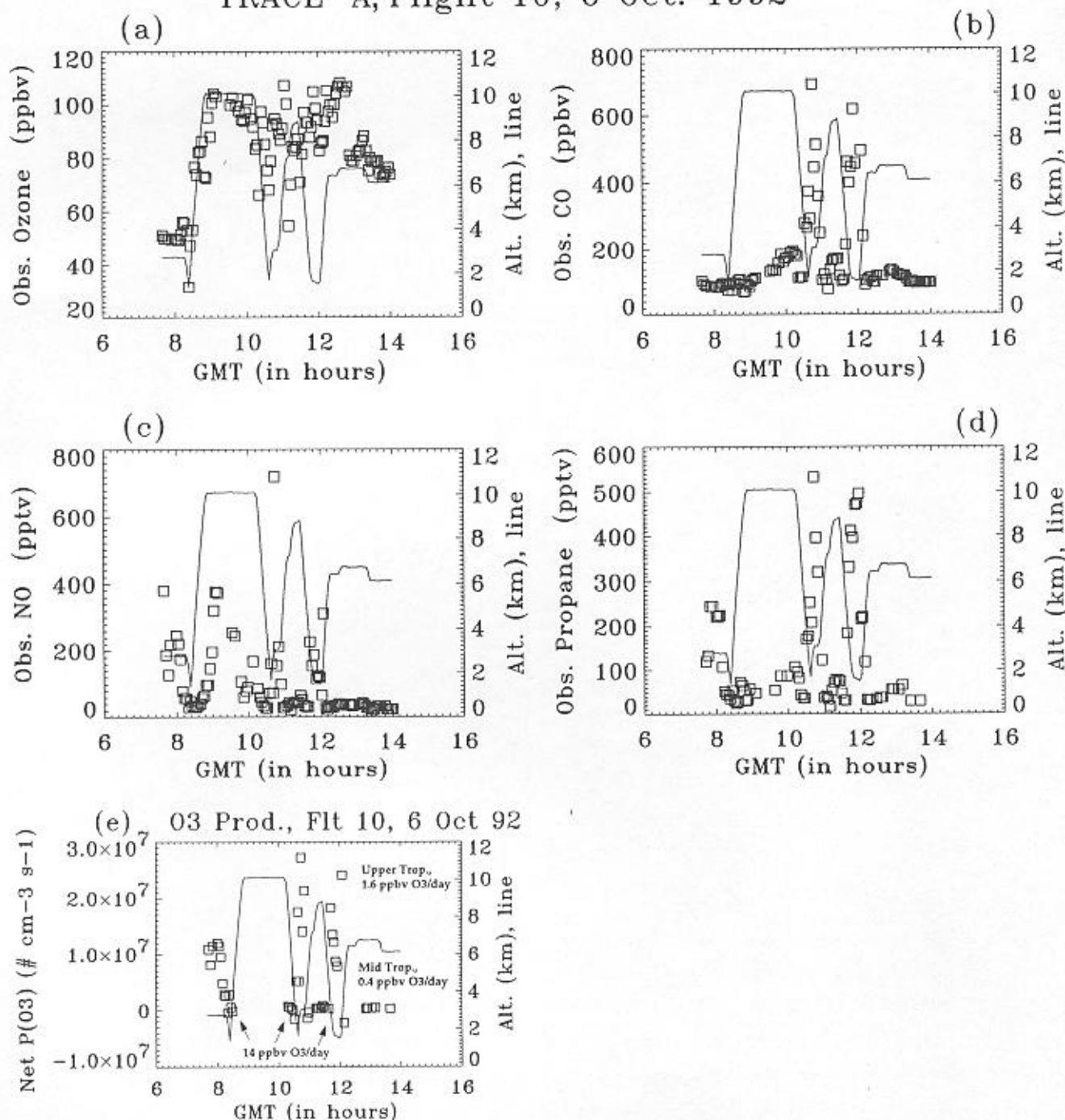


Figure 13. October 11, 1992, Irene (Pretoria) O<sub>3</sub> sounding showing transport from South America and Africa. M-A-M background (dashed line) refers to mean profile from Irene sondes in March–April–May during 1991–1992. Note slow recirculation of air parcels from biomass burning regions of south central Africa (Plate 3). Starting levels are approximately 12 km (188 mbar), 7 km (407 mbar), and 4.5 km (563 mbar).

rectly, in rapid O<sub>3</sub> formation downwind of deep convection and lightning. However, Smyth *et al.* [this issue] point out cases for which a surface, nonbiomass burning NO source is also consistent with species correlations. At Okaukuejo, isotopic tracers from filter samples showed that near-surface ozone might originate from biogenic and localized industrial sources as well as biomass burning (R. J. Swap, personal communication, 1995). Figure 16 is suggestive of lightning, as was upper tropospheric sampling on flight 10. Localized NO maxima (a sudden increase of 50% or more; Figure 16c) are not always correlated with CO (or hydrocarbon) maxima.

Table 5 shows that midtropospheric net O<sub>3</sub> formation rates are always small but variable in sign. This is not surprising given that Atlantic sampling [cf. Browell *et al.*, this issue] showed air parcels of highly variable composition with respect to ozone, aerosols, and ozone precursors [Browell *et al.*, this issue; Gregory *et al.*, this issue]. Ozone and precursor concentrations were not necessarily correlated. Layers of high ozone could be aged with respect to a biomass burning source (a week or more) or coincident with biomass burning tracers (e.g., Figure 16).

## TRACE A, Flight 10, 6 Oct. 1992



**Figure 15.** Sampling of DC-8 data on flight 10 (October 6, 1992) used in GSFC photochemical point model. (a) O<sub>3</sub>, (b) CO, (c) NO, (d) propane. From merged data set prepared by G. Gardner and D. Jacob [Jacob *et al.*, this issue]. (e) Instantaneous net O<sub>3</sub> production for flight 10, evaluated by constraining model with measured mixing ratios of O<sub>3</sub>, CO, NO, hydrocarbons, H<sub>2</sub>O, UV flux, and temperature measured on DC-8 as described in text. Low-altitude legs in active Zambian burning region show equivalent net formation rate 14 ppbv O<sub>3</sub>/d (4 DU/d integrated from 0 to 4 km). This value is obtained by time-weighted averaging of the individual points with accounting for diurnal variation. In the 4–8 km layer, O<sub>3</sub> production is only 0.4 ppbv/d, but at 8–12 km, it increases to 1.6 ppbv O<sub>3</sub>/d.

#### 4.3. Flight 6, September 27, 1992, Brasilia Convective Outflow

We have performed chemical and dynamical analysis of more than a half-dozen convective systems, focusing on the O<sub>3</sub>

forming consequences of individual clouds [Pickering *et al.*, 1992a, b, 1994]. Comparing ozone formation with and without deep convection suggested that convective transport could increase free tropospheric O<sub>3</sub> formation by an order of

## TRACE A, Flt 15, 18 Oct 92

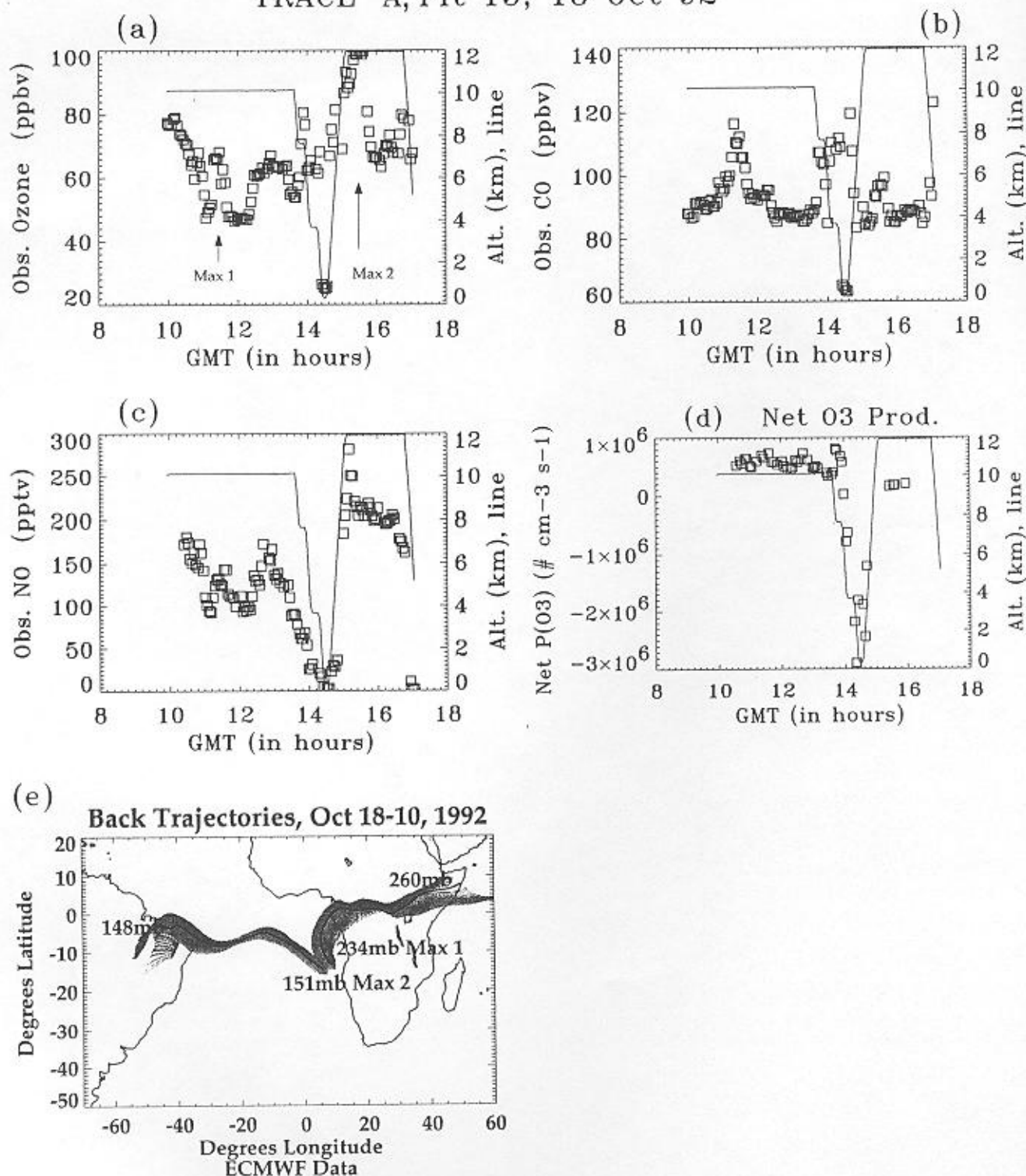
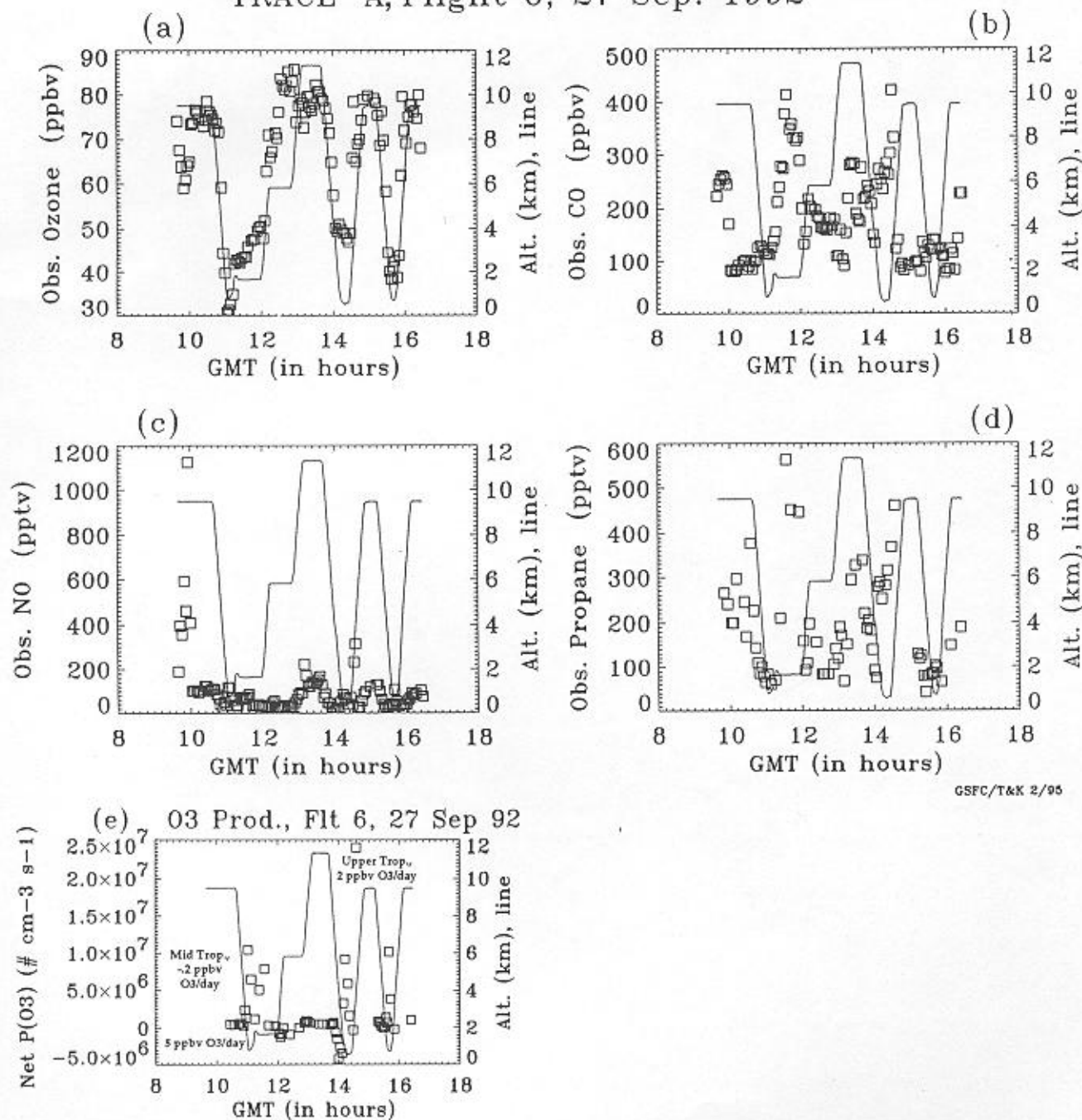


Figure 16. (a) Ozone (b) CO, (c) NO, observations, from Harvard merged data set [Jacob *et al.*, this issue], recorded on flight 15, Atlantic outflow-convergence flight on October 18, 1992. Solid line is altitude. (d) Net O<sub>3</sub> formation rate, computed by GSFC point model. (e) Back trajectories run with ECMWF winds with GSFC isentropic trajectory model from location of two local maxima in Figure 16a. South American source indicated from higher-altitude leg, African source from 10 km. Note net O<sub>3</sub> loss in boundary layer below persistent marine stratocumulus.

## TRACE A, Flight 6, 27 Sep. 1992



GSFC/T&amp;K 2/95

**Figure 17.** DC-8 data on flight 6 (September 27, 1992): (a) O<sub>3</sub>, (b) CO, (c) NO, (d) propane. (e) Instantaneous net O<sub>3</sub> formation as computed with GSFC point model (compare Figure 15). Upper troposphere is O<sub>3</sub>-producing at 1–2 O<sub>3</sub> ppbv/d, as on flights 6 and 15. Convective transport and possibly lightning supply upper troposphere NO<sub>x</sub>. Forward trajectories from flight 6 cloud-outflow levels shown in Figure 10.

magnitude or more [Pickering *et al.*, 1994]. None of these case studies were based on postconvective sampling in cloud outflow air.

Flight 6, September 27, 1992, provided direct observation of convective enhancement of O<sub>3</sub> precursors and (temporary) suppression of O<sub>3</sub> as biomass-burning-influenced air was pumped up through a major mesoscale system that passed across Brazil from September 25 to 28. Details of the observations, with photochemical and dynamical analyses, appear in

the work of Pickering *et al.* [this issue, 1996a] and Wang *et al.* [this issue]. Point modeling is summarized in Figure 17 and Table 5. The main points of Figure 17 are increases in CO above background level (90 ppbv), also in NO and hydrocarbons, with a decrease in O<sub>3</sub>, which is lower in the boundary layer than in the upper troposphere. Like flight 10, the fire-affected boundary layer is net O<sub>3</sub>-producing more so than the free troposphere. Selected data from cloud outflow levels were run in the GSFC point model; this gave 3–4 ppbv O<sub>3</sub>/d forma-

**Table 6.** Selected Natal and Ascension Soundings and Origins

Sounding Date	Total Tropospheric O <sub>3</sub> (0–15 km, DU)	Tropospheric O <sub>3</sub> (10–15 km, DU)	% Excess (10–15 km) of South American Origin
<i>Natal</i>			
March–May, reference	31.5	7.8	...
September 30, 1992	58.7	13.2	20
<i>Ascension</i>			
March–May, reference	29.6	6.6	...
October 3, 1992	52.5	10.4	17
October 5, 1992	49.3	10.6	20

tion with NO mixing ratios averaging 160 pptv. However, for an air parcel with lightning-generated NO averaging 400 pptv, the GSFC box model shows 6–7 ppbv O<sub>3</sub>/d formation [Pickering *et al.*, this issue (a)].

Forward trajectories from the locations of two cloud-outflow layers sampled by the DC-8, starting on September 27, 1992, are shown in Figure 10b. Figures 10 and 11 show the effects of this outflow in soundings over Natal (September 30, 1992) and at Ascension in 4–6 days. Natal soundings show a 10–20 ppbv O<sub>3</sub> increase in levels above 8 km between September 28 and 30 (Figure 10a), consistent with photochemical formation at 5 ppbv O<sub>3</sub>/d. Maxima at Ascension (Figure 11a) span a broader altitude range and are not uniquely traceable to the September 27 event. More likely, they reflect repeated convective injections of O<sub>3</sub>-producing air into the upper troposphere. For Natal and Ascension soundings, the South American contribution to excess O<sub>3</sub> (as defined in section 3.4) is estimated as follows: The cumulative O<sub>3</sub> column depth is computed at 1-km intervals for each profile and “total excess O<sub>3</sub>” obtained by subtracting “background tropospheric O<sub>3</sub>” from the reference profile (Table 4). The “10- to 15-km excess ozone” is also computed; for example, 5.4 DU for September 30, 1992, at Natal is equal to 13.2–7.8 DU along with the fraction, 10–15 km excess/total excess (in percent) (Table 6). Fractions of excess O<sub>3</sub> ascribed to (convective) South American origin are lower limits for profiles in which some back trajectories originate in recirculating patterns with no way to determine the ultimate origin. The 0- to 5-km segment of all 17 Ascension profiles taken in SAFARI/TRACE A originates from Africa, but the midtroposphere appears African in origin for eight profiles, Brazilian in two or three, with the remainder indeterminate.

## 5. Discussion: Regional Ozone Origins During SAFARI/TRACE A

The dynamical and chemical analyses described above are applied to the final set of questions posed in the Introduction: namely, can 40–60 DU tropospheric O<sub>3</sub> over the South Atlantic basin be accounted for by the dynamical and photochemical patterns observed during SAFARI and TRACE A?

### 5.1. Photochemical-Dynamical Interaction

The analysis of section 4 supports an affirmative answer with respect to O<sub>3</sub> photochemical sources [see also Jacob *et al.*, this issue] although Table 5 shows that O<sub>3</sub> photochemical formation rates are only moderate. Contrast the 10–20 ppbv O<sub>3</sub>/d rate near biomass fires with urban-influenced rural sites in industrialized countries. Both O<sub>3</sub> mean mixing ratio and formation rates in the boundary layer of rural summertime North America are 2–3 times the rates shown in Table 5 [Trainer *et al.*, 1987]. TRACE A took place in the latter part of the

biomass burning season, when NO<sub>x</sub>, hydrocarbon, and CO burning sources may have been less than at peak, but satellite climatology shows September and October Atlantic O<sub>3</sub> to be generally higher than in June and July [Fishman *et al.*, 1992]. Some O<sub>3</sub> buildup over the southern Atlantic basin takes place because O<sub>3</sub> photochemical lifetimes in the middle and upper troposphere are 2 weeks or greater. This is confirmed by extensive sampling, DC-3 in southern Africa, DC-8 continental outflow flights, and numerous soundings, that showed high-O<sub>3</sub> layers, frequently <100 m thick, suggesting great stability. Garstang *et al.* [this issue] showed from Irene rawinsondes that horizontal layers below 7 km may be stable in the vertical for more than a month. In general, this behavior characterized lower and midtropospheric structure south of 20°S during SAFARI/TRACE A [Tyson *et al.*, 1996].

A similar picture emerges from the trajectory climatology (section 3). Air masses over southern Africa and the tropical Atlantic recirculate very slowly. Plate 3 showed that only a small fraction of parcels initialized at African fire locations in early October 1992 left the continent after 8 days. The exception is south of 15°S, where fire emissions flow toward the Indian Ocean, a phenomenon confirmed by O<sub>3</sub> soundings at Réunion Island. Even from upper levels over equatorial Africa, where convective outflow is expected, 8-day transport showed little migration beyond the continent. This suggests that O<sub>3</sub> over Africa accumulates as a steady supply of biomass burning fueled O<sub>3</sub> recirculates in the lower and midtroposphere.

Figure 18 is a schematic of ozone photochemical and dynamic interaction over the TRACE A region. Recirculation of air over Africa and the eastern Atlantic, trapped by the dominant anticyclone, supplies the South Atlantic basin with O<sub>3</sub> at low and midtropospheric levels. Robust rates of O<sub>3</sub> formation, based on TRACE A flight 10 and SAFARI DC-3 modeling, are indicated over southern Africa. Near-active fires, O<sub>3</sub> formation throughout the troposphere corresponds to 6 DU/d (0–12 km, Table 5). At this rate, air parcels recirculating in region 2 (Plate 3a) and reexposed to fresh emissions could build up 30–35 DU over fires over 5–6 days. Given that background tropospheric O<sub>3</sub> at this latitude is 25–30 DU (Table 4), tropospheric O<sub>3</sub> column could reach 55–65 DU. At 10°–14°S, 35°E, TOMS shows 50 DU from October 6 to 21, 1992 (Plate 1), and flight 10 UV-DIAL sampling shows 50–55 DU (Figure 2). Thus biomass burning sources, adding to background O<sub>3</sub>, can account for 40–60 DU O<sub>3</sub> over southern Africa. Given the mean lifetime of this O<sub>3</sub> (2–3 weeks), transport in the easterlies supplies the Atlantic and even eastern South America.

Over South America, where deep convection from biomass burning regions appeared to be very effective, O<sub>3</sub> does not accumulate in the lower and midtroposphere, even though

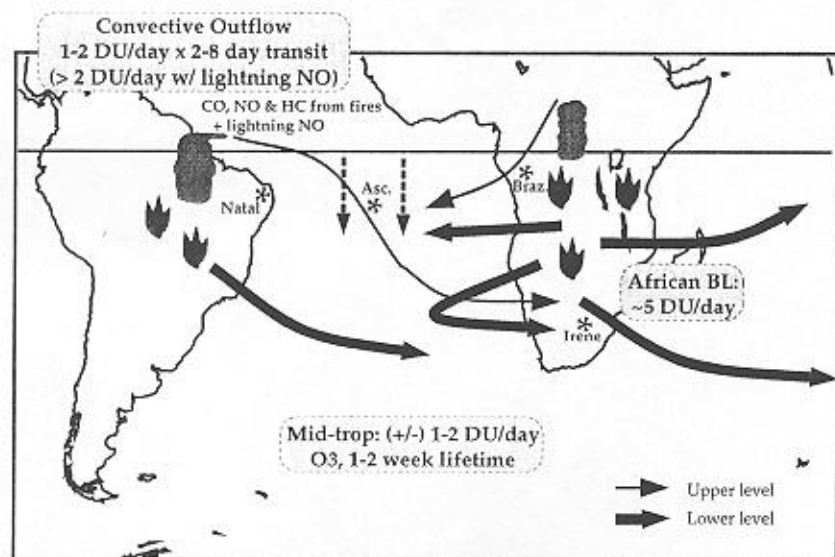


Figure 18. Schematic showing integrated photochemical-transport view of  $O_3$  formation over South Atlantic basin during SAFARI/TRACE A. Ozone formation processes indicated schematically, with downward arrows indicating subsidence over central Atlantic.

flight 6 sampling suggests photochemical  $O_3$  formation rates could be comparable to those over Africa. The mean  $O_3$  concentration from Brazilian flights 5–7 up to 4 km is 46 ppbv compared to 75 ppbv  $O_3$  in the mixed layer over Africa (composite of DC-3 and DC-8 samples). However, cloud-outflow layers from South America have moderately high  $O_3$  formation rates. Based on flight 6, 6–7 ppbv/d adds up to 4 DU in the 8- to 12-km layer during a typical transit across the Atlantic (Figure 18).

Midtropospheric ozone formation over southern Africa and the Atlantic is more variable, ranging between  $-1$  and  $+1$  ppbv  $O_3$ /d. Slow ozone formation may be important to the  $O_3$  climatology under certain conditions, e.g., in air that leaves Africa in the easterlies, or that recirculate slowly over the Atlantic. Five–six days at a 0.5–1 DU/d rate would lead to a 2.5–6 DU layer. This may be one reason why, despite 40-DU  $O_3$  column depth over the continents (Plate 1, Table 3), the Atlantic had more  $O_3$  during October 1992 than Africa or Brazil. A second reason is descent in the central tropical Atlantic from the Walker circulation (downward arrows in Figure 18). High ozone concentrations persist in Ascension soundings from the surface to 5 km (Table 4, Figure 5a), even though the  $O_3$  lifetime in the marine boundary layer is a week or less and Ascension is typically a week from African source regions (Figures 9 and 12a). Excess ozone in the 0- to 5-km layer (Table 4) is greater at Ascension than at Natal and Brazzaville.

Plate 5, a composite of all tropical Atlantic UV-DIAL flights [Browell *et al.*, this issue] shows descension at Ascension and is, in general, a striking corroboration of the mechanisms shown in Figure 18. From South America to Africa (50°W to 30°E) the upper troposphere is enriched with  $O_3$ , but only at longitudes corresponding to Africa and the central Atlantic did the UV-DIAL detect lower and midtropospheric  $O_3 > 60$  ppbv. Plate 5 suggests easterly transport at midtropospheric level across the Atlantic, consistent with an African/Atlantic origin of middle- and low-level  $O_3$  in Natal soundings.

## 5.2. Deep Convection and Relative Contributions of Africa and South America to Atlantic Ozone

Satellite cloud maps, trajectories from convective regions and from fires, analysis of upper tropospheric ozone from the

DC-8 and from sondes, as well as the flight 6 case study all imply a major role for deep convection in ozone formation over the South Atlantic basin during SAFARI/TRACE A. Upper tropospheric correlations by Smyth *et al.* [this issue], Talbot *et al.* [this issue], and Singh *et al.* [this issue] show surface origins common to the insoluble tracers (PAN, hydrocarbons,  $NO_2$ , CO). However, a reactive nitrogen census and elevated levels of NO throughout the upper troposphere are interpreted as lightning [Singh *et al.*, this issue]. Deep convection in South America appears to be responsible for upper tropospheric  $O_3$  enrichment in the majority of soundings at Natal, Ascension, and Okaukuejo. At Brazzaville, convective outflow from Africa (perhaps followed by recirculation over the eastern Atlantic-Gulf of Guinea area) appeared to supply  $O_3$  in the highest- $O_3$  soundings,  $>45$  DU in the period up to October 10, 1992. Farther south, at Okaukuejo and Irene, air parcels at 10–15 km that passed over South America south of 20°S may have transported high ozone from the Pacific or picked up convectively injected South American urban pollution. Even one of the five Réunion soundings during SAFARI/TRACE A with upper tropospheric  $O_3 > 80$  ppbv showed transport at 12.5 km from South American regions with active convection and biomass burning.

Excess ozone for each 5-km layer for each sounding was assigned an origin. In cases of diverging clusters of parcels, excess  $O_3$  was apportioned among several sources. The fraction of excess ozone from each sector, Africa, Atlantic, South America, was computed from total excess  $O_3$  for each sounding. Averages over the September 15 to October 24, 1992, period are given in Table 7. The fraction of African contribution is highest at sites with latitude corresponding to maximum easterly flow and biomass burning. The Atlantic fraction at Okaukuejo and Irene includes trajectories with relatively clean marine air as well as air parcels elevated in  $O_3$  for which complex recirculation patterns preclude unambiguous source assignment.

Most of the excess  $O_3$  assigned to South America in Table 7 was above 10 km, suggesting that the Atlantic maximum- $O_3$  region (Plate 1) received 20–30% of excess  $O_3$  from this region



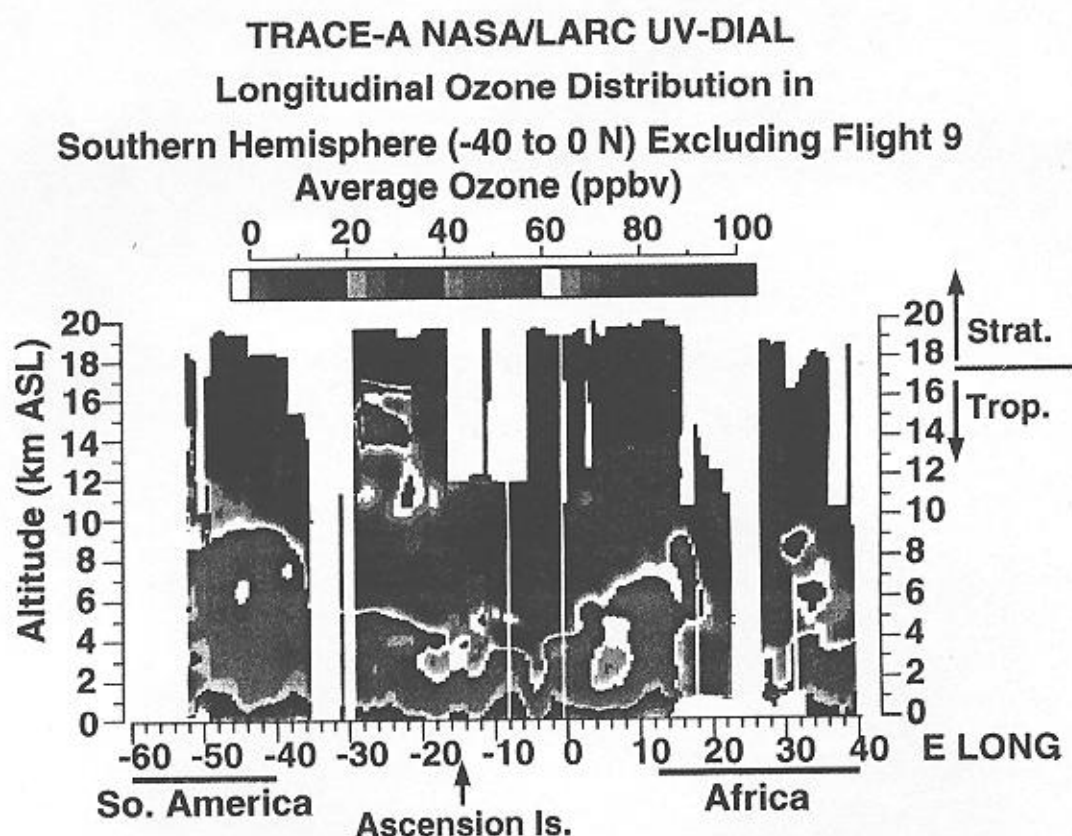


**Plate 5.** Composite, averaged from 0° to 40°S, of UV-DIAL tropospheric O<sub>3</sub> from all TRACE A flights, from South America (50°–60°W) across the Atlantic through southern Africa (20°–30°E) [from *Browell et al.*, this issue].

during SAFARI/TRACE A. Convection over South America and Africa built up in September, as biomass burning declined. For example, *Justice et al.* [this issue] show fire counts in northern Zambia during early October 1992 at 10% or less of July and August 1992 values. The soundings at Ascension, Natal, and Réunion Island show maximum tropospheric O<sub>3</sub> column occurring in September and October; at Brazzaville the O<sub>3</sub> maximum is in August to early September [Thompson *et al.*, this issue; Olson *et al.*, this issue; Baldy *et al.*, this issue]. These patterns may indicate an important role for deep convection. At locations where upper tropospheric O<sub>3</sub> was 20–30% of excess O<sub>3</sub> in October 1992, the buildup in tropospheric O<sub>3</sub> may await the onset of convective activity. There are two aspects to this. First, enhanced O<sub>3</sub> formation in the upper troposphere is brought about by deep convection. Second, once formed, O<sub>3</sub> in the upper troposphere can accumulate due to a relatively long lifetime (Table 5). Olson *et al.* [this issue] note that excess O<sub>3</sub> occurs at higher altitude at Natal than at Ascension and Braz-

zaville. They also note that sources of Atlantic tropospheric O<sub>3</sub> shift from Africa to more of an African-South American mixture as the biomass burning season progresses. Baldy *et al.* [this issue] also speculate that a time lag of several months between maximum biomass fires in Africa and the seasonal tropospheric O<sub>3</sub> maximum at Réunion is due to the onset of frequent deep convection.

## 6. Summary

In this study we used the following data to construct a climatology of tropospheric ozone over southern Africa and the tropical Atlantic O<sub>3</sub> in October 1992 during the GTE TRACE A and SAFARI 1992 field experiments: ozonesondes at four continental and two island sites, a new TOMS tropospheric column O<sub>3</sub> product; in situ and UV-DIAL O<sub>3</sub> measurements from the NASA DC-8 and in situ data from the SAFARI 1992 DC-3. The observations show that the tropical Atlantic and

**Table 7.** Source Apportionment of Soundings During SAFARI/TRACE A (September 15 to October 24, 1992)

Station	Mean Excess Ozone (DU, no.)	African, %	Atlantic, %	So. Am., %
Natal	16.6 (15)	69	3	28
Ascension	19.0 (15)	72	8	20
Brazzaville	10.8 (11)	100	...	...
Okaukuejo	11.1 (15)	62	18	20
Irene	9.3 (15)	48	19	33

adjacent continents are a region of high tropospheric  $O_3$ , with localized maxima  $>50$  DU in column  $O_3$  occurring from southern Africa across to Brazil.

#### Question 1, Ozone Distributions

From soundings and aircraft data the vertical structure of  $O_3$  in southern Africa and the Atlantic is elucidated. Even "clean"  $O_3$  soundings (every site east of the Greenwich meridian had one with total column  $<35$  DU) show multiple layers with up to 40 ppbv variability among adjacent layers. Most aircraft profiles and every sounding site during TRACE A/SAFARI showed layers of high tropospheric  $O_3$ , i.e.  $\geq 90$  ppbv  $O_3$  compared to "background" mixing ratios of 30–40 ppbv, in air masses unaffected by the stratosphere [cf. *Browell et al.*, this issue].

#### Question 2, Ozone and Transport

Trajectories, run backward from the highest- $O_3$  region over the Atlantic (includes Ascension Island), showed direct links to biomass burning regions in Africa and South America. Conversely, forward trajectories from African biomass fire sites during October 1–15, 1992, confirm that  $O_3$ -rich air recirculates over the continent at low (700 mbar) levels, affecting sounding sites removed from burning, e.g., Irene, Okaukuejo. Transport beyond Africa heads in a narrow band toward the Atlantic, where elevated  $O_3$  is registered at Ascension and Natal. South of 15°S, flows are to the east, especially from Mozambique fires, resulting in high  $O_3$  over Réunion.

Forward trajectories, run from cloud outflow level above a South American grid with active fires from September 25 to October 20, 1992, showed rapid flow to the Atlantic, with trajectory parcels over 8 days distributed over the Ascension, Okaukuejo, and Irene sounding sites. Trajectory distributions reflect the dominant meteorology of the TRACE A region in October 1992. The Atlantic or Angolan/Atlantic anticyclone caused stagnation and recirculation in southern Africa and the eastern Atlantic. An intense early wet season, with frequent deep convection over a widespread region of South America, controlled upper troposphere transport.

#### Question 3, Photochemical Sources

The trajectory study supports a biomass-burning-ozone connection, but aircraft observations of  $O_3$ ,  $O_3$  precursors, and tracers are needed to prove a photochemical source. Airborne  $O_3$ , CO,  $NO_x$ , and hydrocarbon data, assimilated into a steady state point model, show that near active burning in Brazil and southern Africa,  $O_3$  is formed photochemically up to 15 ppbv  $O_3/d$ , integrated to 4 DU/d to 4 km. In the upper troposphere, with NO levels frequently at a few hundred pptv (from transformation of  $NO_y$ -reservoir species and/or lightning),  $O_3$  production remains positive, 0.5–3 ppbv  $O_3/d$  or 0.5–1 DU/d [cf. *Jacob et al.*, this issue]. Downwind from convective outflow, selected layers produce even more ozone, 6–7 ppbv  $O_3/d$ . Biogenic ozone sources could be significant in the mixed layer [*Swap et al.*, this issue], but there were insufficient observations to quantify this contribution.

#### Question 4, Synthesis of Mechanisms, Role of Convective Transport, Ozone Origins

In October 1992, southern African and Atlantic tropospheric  $O_3$  achieved a column thickness of 10–30 DU above background (nonburning season column depth) due to a unique interaction of meteorology and photochemistry. Over

Africa, robust  $O_3$ -forming rates, combined with low wind speeds, extensive recirculation, and stable layering cause an  $O_3$  buildup throughout the lower and middle troposphere. Easterlies and continued recirculation over the Atlantic led to  $O_3$  enrichment detected by the DC-8 and Natal and Ascension soundings; slow  $O_3$  formation continued in the upper troposphere during transport. The importance of deep convective transport as a mechanism for supplying upper tropospheric  $O_3$  was confirmed in TRACE A (flight 6) and in downwind  $O_3$  soundings. Deep convective transport from South America was responsible for 20–30% of the excess tropospheric  $O_3$  burden over the South Atlantic basin during SAFARI/TRACE A. Convective outflow from southern Africa supplied upper tropospheric ozone and/or ozone precursors to Brazzaville and Réunion.

We comment on other questions of TRACE A and SAFARI. How much  $O_3$  is from biomass burning and how much is from other sources? Further analysis with correlations, tracers, etc., is needed. SAFARI scientists measured significant biogenic fluxes for NO and CO under certain conditions; the present study, based on ambient mixing ratios, not fluxes, does not address biogenic sources. Was October 1992 typical for South Atlantic ozone during this time of year? The extreme drought in southern Africa reduced biomass burning in that area, but north of 20°S, biomass burning was close to normal [*Justice et al.*, this issue]. Cloud, precipitation, and  $O_3$  characteristics observed in Brazil suggest that in other years, transport from this region might be lower than in October 1992.

Two aspects of South Atlantic ozone origins deserve emphasis. One is that although ozone precursors are abundant (from biomass burning, biogenic sources, and/or lightning), the particular dynamics of the South Atlantic are essential to the ozone buildup. Other tropical areas have extensive biomass burning, e.g., Southeast Asia, but no comparable ozone signature [*Fishman et al.*, 1991]. Second, the TRACE A finding that upper tropospheric NO levels are robust enough to maintain steady  $O_3$  formation and that lightning is a key, if not a dominant cause, call for further investigation. Satellite lightning maps, e.g., as supplied by the optical transient detector, launched in 1995 (H. Christian, personal communication, 1996), will be invaluable in this regard.

**Acknowledgments.** It is a pleasure to acknowledge the support of the GTE TRACE A Project and the NASA Tropospheric Chemistry, Atmospheric Chemical Modeling and Analysis (ACMAP), EOS programs and EPA interagency agreements (DW8093-6126 and 8093-6290). This work benefited greatly from collaboration with TRACE A and SAFARI 1992 scientists, in particular D. Jacob, J. Logan, J. Bradshaw, G. Gregory, G. Sachse, D. Blake, W. Grant, M. Andreae, T. Zenker, G. Helas, R. Diab, M. Garstang, P. Tyson, G. Bodeker, and G. Coetzee. Thanks to the U. Natal Students Visiting Travel Fund for partial travel support in Africa in 1993. J. Fishman and V. Brackett (SAIC, Langley Research Center) and J. Kendall (SSAI, NASA Goddard) provided ozonesonde and fire-count data. T. Kucsera (Applied Research Corporation, NASA Goddard) assisted with point modeling. ISCCP data were obtained from the Langley DAAC.

#### References

- Andreae, M. O., J. Fishman, M. Garstang, J. G. Goldammer, C. O. Justice, J. S. Levine, R. J. Scholes, B. J. Stocks, A. M. Thompson, B. van Wilgen, and the STARE/TRACE-A/SAFARI-92 Science Team, Biomass burning in the global environment: First results from the IGAC/BIBEX field campaign STARE/TRACE-A/SAFARI-92, in *Global Atmospheric-Biospheric Chemistry: The First IGAC Scientific*

- Conference, edited by R. Prinn, pp. 83-101, Plenum, New York, 1994a.
- Andreae, M. O., B. E. Anderson, D. R. Blake, J. D. Bradshaw, J. E. Collins, G. L. Gregory, G. W. Sachse, and M. C. Siphon, Influence of plumes from biomass burning on atmospheric chemistry over the equatorial and tropical South Atlantic during CITE 3, *J. Geophys. Res.*, **99**, 12,793-12,808, 1994b.
- Bachmeier, A. S., and H. E. Fuelberg, A meteorological overview of the TRACE A period, *J. Geophys. Res.*, this issue.
- Baldy, S., G. Ancellet, M. Bessafi, A. Badr, and D. Lan Sun Luk, Field observations of the vertical distribution of tropospheric ozone at the Island of La Reunion (southern tropics), *J. Geophys. Res.*, this issue.
- Browell, E. V., et al., Ozone and aerosol distributions and air mass characteristics observed over the South Atlantic basin during the burning season, *J. Geophys. Res.*, this issue.
- Brunke, E.-G., H. E. Scheel, and W. Seiler, Trends of tropospheric CO, N<sub>2</sub>O, and CH<sub>4</sub> as observed at Cape Point, South Africa, *Atmos. Environ.*, **24A**, 585-595, 1990.
- Chatfield, R. B., J. A. Vastano, H. B. Singh, and G. Sachse, A general model of how fire emissions and chemistry produce African/oceanic plumes (O<sub>3</sub>, CO, PAN, smoke) in TRACE A, *J. Geophys. Res.*, this issue.
- Cofe, W. R., III, J. S. Levine, E. L. Winstead, D. R. Cahoon, D. I. Sebach, J. P. Pinto, and B. J. Stocks, Source compositions of trace gases released during African savanna fires, *J. Geophys. Res.*, this issue.
- Cros, B., D. Nganga, A. Minga, J. Fishman, and V. Brackett, Distribution of tropospheric ozone at Brazzaville, Congo, determined from ozonesonde measurements, *J. Geophys. Res.*, **97**, 12,869-12,876, 1992.
- Diab, R., et al., Vertical ozone distribution over southern Africa and adjacent oceans during SAFARI 1992, *J. Geophys. Res.*, this issue (a).
- Diab, R. D., M. R. Jury, J. M. Combrink, and F. Sokolic, A comparison of anticyclone and trough influences on the vertical distribution of ozone and meteorological conditions during SAFARI 1992, *J. Geophys. Res.*, this issue (b).
- Fabian, P., and R. G. Pruchniewicz, Meridional distribution of ozone in the troposphere and its seasonal variations, *J. Geophys. Res.*, **82**, 2063-2073, 1977.
- Fishman, J., Tropospheric ozone from satellite total ozone measurements, in *Tropospheric Ozone*, edited by I. S. A. Isaksen, pp. 111-123, D. Reidel, Norwell, Mass., 1988.
- Fishman, J., Experiment probes elevated ozone levels over the tropical South Atlantic Ocean, *Eos Trans. AGU*, **75**, 38, 1994.
- Fishman, J., P. Minnis, and H. G. Reichle Jr., The use of satellite data to study tropospheric ozone in the tropics, *J. Geophys. Res.*, **91**, 14,451-14,465, 1986.
- Fishman, J., C. E. Watson, J. C. Larsen, and J. A. Logan, The distribution of tropospheric ozone determined from satellite data, *J. Geophys. Res.*, **95**, 3599-3617, 1990.
- Fishman, J., K. Fakhruzzaman, B. Cros, and D. Nganga, Identification of widespread pollution in the Southern Hemisphere deduced from satellite analyses, *Science*, **252**, 1693-1696, 1991.
- Fishman, J., V. G. Brackett, and K. Fakhruzzaman, Distribution of tropospheric ozone in the tropics from satellite and ozonesonde measurements, *J. Atmos. Terr. Phys.*, **54**, 589-597, 1992.
- Fishman, J., J. M. Hoell Jr., R. D. Bendura, V. W. J. H. Kirchhoff, and R. J. McNeal Jr., NASA GTE TRACE A experiment (September-October 1992): Overview, *J. Geophys. Res.*, this issue (a).
- Fishman, J., V. G. Brackett, E. V. Browell, and W. B. Grant, Tropospheric ozone derived from TOMS/SBUV measurements during TRACE A, *J. Geophys. Res.*, this issue (b).
- Fuelberg, H. E., R. O. Loring, Jr., M. V. Watson, M. C. Sinha, K. E. Pickering, A. M. Thompson, G. W. Sachse, D. R. Blake, and M. R. Schoeberl, TRACE A trajectory intercomparison, 2, Isentropic and kinematic methods, *J. Geophys. Res.*, this issue.
- Garstang, M., and P. D. Tyson, Atmospheric circulation, vertical structure and transport, chap. 6, in *Fire in Southern African Savanna: Ecological and Atmospheric Perspectives*, edited by B. W. van Wilgen, M. S. Andreae, and J. G. Goldammer, and J. A. Lindsay, Univ. Witwatersrand Press, Johannesburg, in press, 1996.
- Garstang, M., P. D. Tyson, R. Swap, M. Edwards, P. Källberg, and J. A. Lindsay, Horizontal and vertical transport of air over southern Africa, *J. Geophys. Res.*, this issue.
- Gregory, G. L., H. E. Fuelberg, S. F. Longmore, B. E. Anderson, J. E. Collins, and D. R. Blake, Chemical characteristics of tropospheric air over the tropical South Atlantic Ocean: Relationship to trajectory history, *J. Geophys. Res.*, this issue.
- Harris, G. W., F. G. Wienhold, and T. Zenker, Airborne observations of strong biogenic NO<sub>x</sub> emissions from the Namibian savanna at the end of the dry season, *J. Geophys. Res.*, this issue.
- Heikes, B. G., M. Lee, D. J. Jacob, R. Talbot, J. D. Bradshaw, H. B. Singh, D. R. Blake, B. E. Anderson, H. E. Fuelberg, and A. M. Thompson, Ozone, hydroperoxides, oxides of nitrogen, and hydrocarbon budgets in the marine boundary layer over the South Atlantic, *J. Geophys. Res.*, this issue.
- Hovmöller, E., The trough-and-ridge diagram, *Tellus*, **1**, 62-66, 1949.
- Hudson, R. D., J.-H. Kim, and A. M. Thompson, On the derivation of tropospheric column ozone from radiances measured by the total ozone mapping spectrometer, *J. Geophys. Res.*, **100**, 11,137-11,145, 1995.
- Jacob, D. J., et al., Origin of ozone and NO<sub>x</sub> in the tropical troposphere: A photochemical analysis of aircraft observations over the South Atlantic basin, *J. Geophys. Res.*, this issue.
- Jury, M., E.-G. Brunke, and M. Schormann, Aircraft section measurements of meteorology and ozone in northern Namibia during SAFARI 1992, *J. Geophys. Res.*, this issue.
- Justice, C. O., J. D. Kendall, P. R. Dowty, and R. J. Scholes, Satellite remote sensing of fires during the SAFARI campaign using NOAA AVHRR data, *J. Geophys. Res.*, this issue.
- Kim, J. H., R. D. Hudson, and A. M. Thompson, A new method of deriving time-averaged tropospheric column ozone over the tropics using total ozone mapping spectrometer radiances: Intercomparison and analysis using TRACE A data, *J. Geophys. Res.*, this issue.
- Kirchhoff, V. W. J. H., R. A. Barnes, and A. L. Torres, Ozone climatology at Natal from in situ ozonesonde data, *J. Geophys. Res.*, **96**, 10,899-10,909, 1991.
- Kirchhoff, V. W. J. H., J. R. Alves, F. R. da Silva, and J. Fishman, Observations of ozone concentrations in the Brazilian cerrado during the TRACE A field expedition, *J. Geophys. Res.*, this issue.
- Krishnamurti, T. N., H. E. Fuelberg, M. C. Sinha, D. Osterhof, E. L. Bensman, and V. B. Kumar, The meteorological environment of the tropospheric ozone maximum over the tropical South Atlantic, *J. Geophys. Res.*, **98**, 10,621-10,641, 1993.
- Krishnamurti, T. N., M. C. Sinha, M. Kanamitsu, D. Osterhof, H. Fuelberg, R. Chatfield, D. J. Jacob, and J. Logan, Passive tracer transport relevant to the TRACE A experiment, *J. Geophys. Res.*, this issue.
- Lindsay, J. A., J. G. Goldammer, H. J. Annegarn, R. J. Scholes, M. O. Andreae, G. Harris, M. Garstang, and B. W. van Wilgen, The International Biosphere-Geosphere Program/International Global Atmospheric Chemistry SAFARI 1992, *J. Geophys. Res.*, this issue.
- Logan, J. A., and V. W. J. H. Kirchhoff, Seasonal variations of tropospheric ozone at Natal, Brazil, *J. Geophys. Res.*, **91**, 7875-7881, 1986.
- Meixner, F. X., and G. Helas, Meteorology, transport and boundary layer ozone at Victoria Falls, Zimbabwe, *Eos, Trans. AGU*, **75**, 147, 1994.
- National Meteorological Center (NMC), *Climate Diagnostics Bulletin*, NOAA, Washington, D. C., September and October 1992.
- Nganga, D. A. Minga, B. Cros, B. Bouka Biona, J. Fishman, and W. B. Grant, Vertical distribution of ozone measured at Brazzaville, Congo, during TRACE A, *J. Geophys. Res.*, this issue.
- Olson, J. R., J. Fishman, and V. W. J. H. Kirchhoff, An analysis of the distribution of ozone over the southern Atlantic region, *J. Geophys. Res.*, this issue.
- Pereira, E. B., A. W. Setzer, F. Gerab, P. E. Artaxo, M. C. Pereira, and G. Monroe, Airborne measurements of aerosols from burning biomass in Brazil related to the TRACE A experiment, *J. Geophys. Res.*, this issue.
- Pickering, K. E., A. M. Thompson, J. R. Scala, W.-K. Tao, and J. Simpson, Ozone production potential following convective redistribution of biomass burning emissions, *J. Atmos. Chem.*, **14**, 297-313, 1992a.
- Pickering, K. E., J. R. Scala, A. M. Thompson, W.-K. Tao, and J. Simpson, A regional estimate of convective transport of CO from biomass burning, *Geophys. Res. Lett.*, **19**, 289-292, 1992b.
- Pickering, K. E., A. M. Thompson, J. R. Scala, W.-K. Tao, and J. Simpson, Enhancement of free tropospheric ozone production by deep convection, in *Ozone in the Troposphere and Stratosphere*, edited by R. D. Hudson, *NASA Conf. Publ.* 3266, pp. 105-108, 1994.
- Pickering, K. E., et al., Convective transport of biomass burning emissions over Brazil during TRACE A, *J. Geophys. Res.*, this issue (a).

- Pickering, K. E., A. M. Thompson, D. P. McNamara, M. R. Schoeberl, H. E. Fuelberg, R. E. Loring, M. V. Watson, K. Fakhruzzaman and A. S. Bachmeier, TRACE A trajectory intercomparison, 1, Effects of different input analyses, *J. Geophys. Res.*, this issue (b).
- Scheel, H.-E., R. Sladkovic, E.-G. Brunke, and W. Seiler, Measurements of lower tropospheric ozone at midlatitudes of the northern and southern hemisphere, in *Ozone in the Troposphere and Stratosphere*, edited by R. D. Hudson, NASA Conf. Publ. 3266, 11-14, 1994.
- Schoeberl, M. R., L. R. Lait, P. A. Newman, and J. S. Rosenfield, The structure of the polar vortex, *J. Geophys. Res.*, 97, 7859-7882, 1992.
- Scholes, R. J., D. Ward, and C. O. Justice, Emissions of trace gases and aerosol particles due to vegetation burning in southern hemisphere Africa, *J. Geophys. Res.*, this issue.
- Singh, H. B., et al., Impact of biomass burning emissions on the composition of the South Atlantic troposphere: Reactive nitrogen and ozone, *J. Geophys. Res.*, this issue.
- Smyth, S., et al., Factors influencing the upper free tropospheric distribution of reactive nitrogen over the South Atlantic during the TRACE A experiment, *J. Geophys. Res.*, this issue.
- Swap, R. J., M. Garstang, S. A. Macko, P. D. Tyson, W. Maenhaut, P. Artaxo, P. Källberg, and R. Talbot, The long-range transport of southern African aerosols to the tropical South Atlantic, *J. Geophys. Res.*, this issue.
- Swap, R. J., M. Garstang, S. A. Macko, P. D. Tyson, and P. Källberg, Comparison of biomass burning emissions and biogenic emissions to the tropical South Atlantic, in *Biomass Burning and Global Change*, edited by J. S. Levine, MIT Press, Cambridge, Mass., in press, 1996.
- Talbot, R. W., et al., Chemical characteristics of continental outflow over the tropical South Atlantic Ocean from Brazil and Africa, *J. Geophys. Res.*, this issue.
- Thompson, A. M., Evaluation of biomass burning effects on ozone during SAFARI/TRACE-A: Examples from process models, in *Biomass Burning and Global Change*, edited by J. S. Levine, MIT Press, Cambridge, Mass., in press, 1996.
- Thompson, A. M., K. E. Pickering, D. P. McNamara, and R. D. McPeters, Effect of marine stratocumulus on TOMS ozone, *J. Geophys. Res.*, 98, 23,051-23,057, 1993.
- Thompson, A. M., et al., Ozone over southern Africa during SAFARI 1992/TRACE A, *J. Geophys. Res.*, this issue.
- Thompson, A. M., T. Zenker, G. E. Bodeker, and D. P. McNamara, Ozone over southern Africa: Patterns and influences, in *Fire in Southern African Savanna: Ecological and Atmospheric Perspectives*, edited by B. W. van Wilgen, M. Andreae, J. G. Goldammer, and J. A. Lindsay, Univ. Witwatersrand Press, Johannesburg, in press, 1996.
- Trainer, M., E.-Y. Hsie, S. A. McKeen, R. Tallamraju, D. D. Parrish, F. C. Fehsenfeld, and S. C. Liu, Impact of natural hydrocarbons on hydroxyl and peroxy radicals at a remote site, *J. Geophys. Res.*, 92, 11,879-11,894, 1987.
- Tyson, P. D., M. Garstang, R. Swap, P. Källberg, and M. Edwards, An air transport climatology for subtropical southern Africa, *Int. J. Climatol.*, 16, 265-291, 1996.
- van Wilgen, B. W., M. O. Andreae, J. G. Goldammer, and J. A. Lindsay (Eds.), *Fire in Southern African Savanna: Ecological and Atmospheric Perspectives*, Univ. Witwatersrand Press, Johannesburg, in press, 1996.
- Wang, Y., W.-K. Tao, K. E. Pickering, A. M. Thompson, J. S. Kain, R. Adler, J. Simpson, P. Keehn, and G. Lai, Mesoscale model (MM5) simulations of TRACE A and PRESTORM convective systems and associated tracer transport, *J. Geophys. Res.*, this issue.
- Zenker, T., A. M. Thompson, D. P. McNamara, T. L. Kucsera, F. G. Wienhold, G. W. Harris, P. LeCanut, M. O. Andreae, and R. Koppmann, Regional trace gas distribution and air mass characteristics in the haze layer over southern Africa during the biomass burning season (Sep./Oct. 1992): Observations and modeling from the STARE/SAFARI-92/DC-3, in *Biomass Burning and Global Change*, edited by J. S. Levine, MIT Press, Cambridge, Mass., in press, 1996.
- Zepp, R. G., W. L. Miller, R. A. Burke, D. A. B. Parsons, and M. C. Scholes, Effects of moisture and burning on soil-atmosphere exchange of trace carbon gases in a southern African savanna, *J. Geophys. Res.*, this issue.
- Zunckel, M., Y. Hong, and S. O'Beirne, Characteristics of the nocturnal boundary layer at Okaukuejo during SAFARI 1992 (September and October 1992), *J. Geophys. Res.*, this issue.
- E. V. Browell, NASA Langley Research Center, Atmospheric Sciences Division, Hampton, VA 23681.
- R. D. Hudson, and K. E. Pickering, Department of Meteorology, University of Maryland Joint Center for Earth System Science (JCESS), College Park, MD 20742.
- J. H. Kim, Earth System Science Laboratory, University of Alabama, Huntsville, AL 35899.
- V. W. J. Kirchhoff, INPE, São Jose de Campos, São Paulo, Brazil 12-201-970.
- D. P. McNamara, Applied Research Corporation, 8201 Corporate Drive, Landover, MD 20785.
- D. Nganga, Department of Atmospheric Physics, Marien Ngouabi University, Brazzaville, Congo.
- M. R. Schoeberl and A. M. Thompson (corresponding author), NASA Code 916, Bldg. 21, Room 264, Greenbelt, MD 20771. (e-mail: thompson@gator1.gsfc.nasa.gov)

(Received March 23, 1995; revised May 7, 1996; accepted May 9, 1996.)